

## Diffusible repression of cytokinin signalling produces endodermal symmetry and passage cells

Tonni Grube Andersen<sup>1</sup>, Sadaf Naseer<sup>1</sup>, Robertas Ursache<sup>1</sup>, Brecht Wybouw<sup>2,3</sup>, Wouter Smet<sup>2,3,4</sup>, Bert De Rybel<sup>2,3,4</sup>, Joop E.M. Vermeer<sup>1†</sup> & Niko Geldner<sup>1</sup>

In vascular plants, the root endodermis surrounds the central vasculature as a protective sheath that is analogous to the polarized epithelium in animals, and contains ring-shaped Casparian strips that restrict diffusion<sup>1</sup>. After an initial lag phase, individual endodermal cells suberize in an apparently random fashion to produce ‘patchy’ suberization that eventually generates a zone of continuous suberin deposition<sup>2</sup>. Casparian strips and suberin lamellae affect paracellular and transcellular transport, respectively. Most angiosperms maintain some isolated cells in an unsuberized state<sup>3</sup> as so-called ‘passage cells’, which have previously been suggested to enable uptake across an otherwise-impermeable endodermal barrier<sup>3,4</sup>. Here we demonstrate that these passage cells are late emanations of a meristematic patterning process that reads out the underlying non-radial symmetry of the vasculature. This process is mediated by the non-cell-autonomous repression of cytokinin signalling in the root meristem, and leads

to distinct phloem- and xylem-pole-associated endodermal cells. The latter cells can resist abscisic acid-dependent suberization to produce passage cells. Our data further demonstrate that, during meristematic patterning, xylem-pole-associated endodermal cells can dynamically alter passage-cell numbers in response to nutrient status, and that passage cells express transporters and locally affect the expression of transporters in adjacent cortical cells.

For more than a century, it has been known that angiosperm roots display interspersed passage cells in their suberized endodermis<sup>4</sup>. In monocots, these cells remain thin-walled and unsuberized for many months<sup>4</sup>, which suggests that passage cells represent a stable cell fate. In *Arabidopsis*, passage cells have only sporadically been mentioned and the scarce experiments that have addressed the function of these cells have mostly been correlative<sup>3,5</sup>. Although the molecular basis of passage cell development is as yet unknown, suberization in *Arabidopsis* follows a stereotypic pattern<sup>2</sup> that has recently been shown to be highly

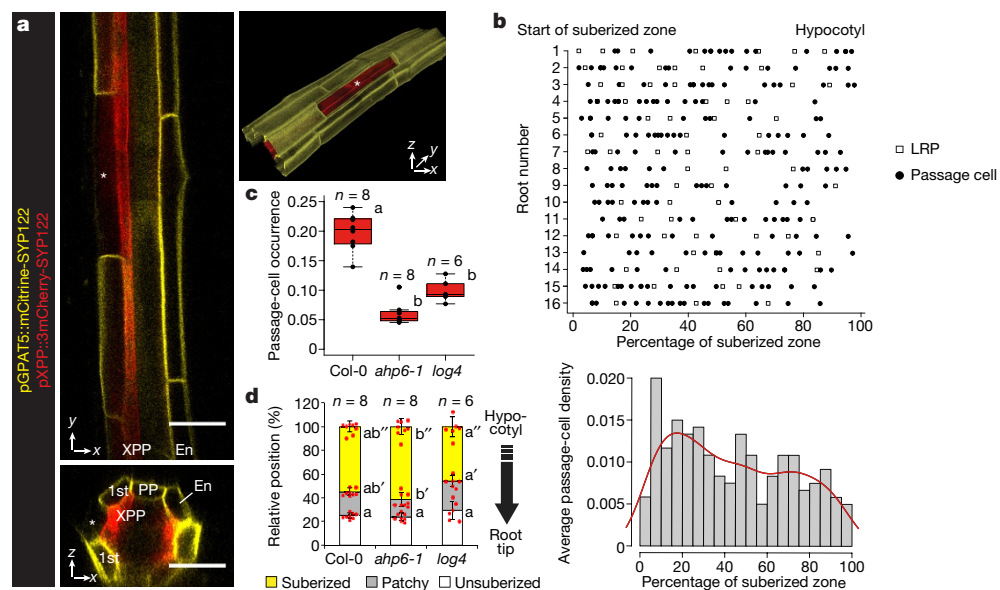


**Figure 1 | Presence and distribution of passage cells in *Arabidopsis*.**

**a**, Representative suberized endodermis and xylem-pole pericycle visualized by a suberin (*GPAT5*) and xylem-pole pericycle (XPP) reporter, using plasma-membrane-localized mCitrine-SYP122 or 3mCherry-SYP122 reporters, respectively. Asterisk, passage cell. **b**, Top, scoring of lateral root primordia (white squares) and passage cells (black circles) from the start of the fully suberized zone (0%) to the hypocotyl junction (100%). Bottom, 5% binning of data from top panel (grey bars), and trend of passage-cell density along the suberized zone (red line). **c**, Passage-cell occurrence in Col-0 plants, and *ahp6-1* and *log4* mutants. **d**, Suberization in Col-0 plants, and *ahp6-1* and *log4* mutants. En, endodermis;

PP, phloem pole. Bar graphs represent mean  $\pm$  s.d. and boxplot centres show median. In all graphs, dots represent individual data points. For all stacked graphs, there are three measurements per root: unsuberized zone, white; patchy zone, grey; and suberized zone, yellow. Individual letters show significantly different groups according to a post hoc Bonferroni-adjusted paired two-sided *t*-test. The prime symbols indicate that *t*-tests were performed on measurements within identical zones, that is two primes for suberized, one prime for patchy and none for unsuberized. For more information on data plots, see Methods. The image in **a** is representative of five independent lines. *n*, independent biological samples. For individual *P* values, see Supplementary Table 2. Scale bars, 25  $\mu$ m.

<sup>1</sup>Department of Plant Molecular Biology, University of Lausanne, 1015 Lausanne, Switzerland. <sup>2</sup>Ghent University, Department of Plant Biotechnology and Bioinformatics, 9052 Ghent, Belgium. <sup>3</sup>VIB Center for Plant Systems Biology, 9052 Ghent, Belgium. <sup>4</sup>Wageningen University, Laboratory of Biochemistry, 6708 WE Wageningen, The Netherlands. <sup>†</sup>Present address: Department of Plant and Microbial Biology, University of Zürich, 8008 Zürich, Switzerland.

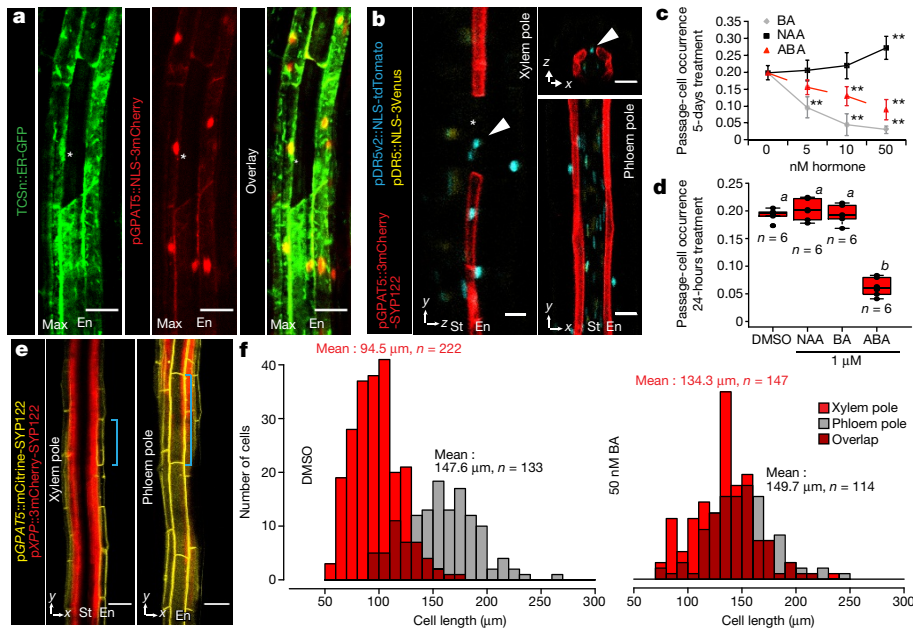


**Figure 2 | Cytokinin and auxin regulate endodermal patterning and passage cell formation.** **a**, Representative image depicting expression of the cytokinin response marker *TCSn* (ER–GFP, green; ER, endoplasmic reticulum) or the suberin reporter *GPAT5* (NLS–3mCherry, red; NLS, nuclear localization signal) in fully suberized endodermis. **b**, Expression of auxin signalling reporter *DR5v2* (NLS–tdTomato, blue), or *DR5* (NLS–3mVenus, yellow) and suberin marker *GPAT5* (3mCherry–SYP122, red) in fully suberized endodermis. Red dots, individual data points. **c**, **d**, Occurrence of passage cells in seedlings germinated on indicated hormones (**c**) or after 24-h hormone incubation (**d**). Dimethyl sulfoxide (DMSO), mock treatment. Black dots, individual data points. **e**, Optical sections through suberized endodermis. Suberin and xylem-pole pericycle highlighted as in Fig. 1a. Blue lines, length of a single cell in xylem or

phloem pole. **f**, Distribution of suberized endodermal cell length in xylem or phloem pole of plants germinated on mock (DMSO) or cytokinin plates. Numbers depict average lengths of xylem-pole (red) or phloem-pole (grey) endodermal cells. Asterisks indicate passage cells and arrowheads indicate passage-cell nuclei. BA, benzyl adenine; NAA, naphthalene acetic acid; Max, maximum projection; St, stele. Boxplot centres show median. Statistically significant differences between groups were tested using a post hoc Bonferroni-adjusted paired two-sided *t*-test. In **a**, **b** and **e**, image is representative of eight independent lines. *n*, independent biological samples. In **c**, *\*\*P* < 0.01, two-tailed *t*-test. Dots represent mean, error bars are s.d. and *n* = 25 independent biological replicas for each treatment. For more information regarding data plots, see Methods. For individual *P* values, see Supplementary Table 2. Scale bars, 25  $\mu$ m.

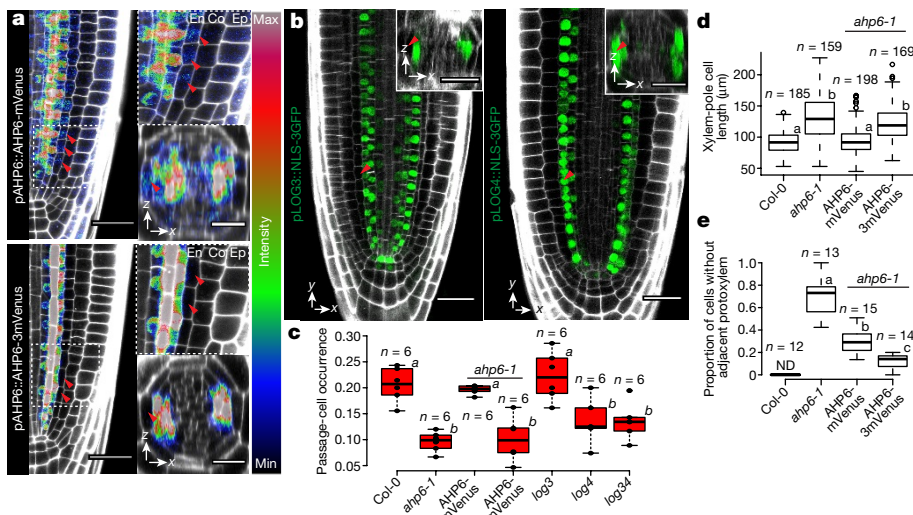


**Figure 3 | Spatially restricted cytokinin repression and production underlie passage cell formation.** **a**, Expression of pAHP6::AHP6-mVenus or pAHP6::AHP6-3mVenus from a previously published line<sup>19</sup> in the root meristem. Figures represent longitudinal and transverse optical sections through the xylem pole of the root meristematic zone. **b**, *pLOG3* and *pLOG4* reporter activity (NLS–3GFP, green) in the root meristem. The lines that we used have previously been published<sup>8</sup>. **c**, Occurrence of passage cells in *ahp6-1* and lines complemented with AHP6 fused to a single or triple mVenus protein, driven from *AHP6* promoter. Dots, individual data points. **d**, Length of xylem-pole endodermal cells in the suberized zone of *ahp6-1* and in lines complemented with AHP6 fusions.

Dots, outliers. **e**, Quantification of xylem defects in *ahp6-1* mutant lines (for details, see Methods). Co, cortex; Ep, epidermis; ND, not detected. Red arrowheads, xylem-pole endodermal cells. Boxplot centres show the median. Statistically significant differences between groups were tested using a post hoc Bonferroni-adjusted paired two-sided *t*-test. For more information on data plots, see Methods. In **a** and **b**, images are representative of previously published lines<sup>8,19</sup>. *n*, independent biological samples. In **d**, *n* represents individual measurements across 16 independent biological samples. For individual *P* values, see Supplementary Table 2. Scale bars, 25  $\mu$ m.

responsive to many stress conditions, mediated by abscisic acid (ABA) and ethylene<sup>2</sup>. In the zone of continuous suberization, we found individual cells that lacked suberin deposition (Fig. 1a), which was reliably paralleled by a live marker for suberization<sup>2</sup> (Extended Data Fig. 1a–c). Using a marker for the xylem-pole pericycle (Extended Data Fig. 1d), we demonstrate a close association between these suberin-lacking cells and the xylem pole (Extended Data Fig. 1f); this close association is a second defining feature of passage cells<sup>3</sup>. Similar to other angiosperms, suberization in *Arabidopsis* begins above the phloem pole, approximately four cells closer to the root tip than above the xylem pole<sup>3</sup> (Extended Data Fig. 1g, h). Although passage cells appear randomly along the longitudinal axis and are not correlated with sites of lateral root emergence, they are sometimes clustered and have a tendency to decrease towards the hypocotyl (Fig. 1b and Extended Data Fig. 1e). To understand the mechanism that determines the association between passage cells and the xylem pole, we investigated mutants of genes involved in xylem patterning. Two cytokinin-related mutants, *ahp6-1* (also known as *hp6-1*) and *log4*, showed reduced numbers of passage cells without affecting overall suberization (Fig. 1c, d). AHP6 attenuates cytokinin responses<sup>6</sup>, and LOG4 is involved in cytokinin biosynthesis<sup>7,8</sup>. Auxin–cytokinin interactions are essential to establish the bisymmetric pattern of phloem and xylem poles<sup>9,10</sup>. The preferential accumulation of auxin in xylem precursors is thought to lead to the expression of AHP6 and LOG4, turning these cells into a cytokinin-refractory cytokinin source. Higher levels of cytokinin signalling in neighbouring cells then induces procambium and/or phloem pole cells<sup>8</sup>, which in turn usher more auxin towards xylem precursors and thereby establish complementary domains of auxin and cytokinin perception<sup>10</sup>. We hypothesized that these bisymmetric signalling domains also cause the association of passage cells with the xylem pole.

Using a cytokinin-response marker<sup>11</sup>, we observed responses in the suberized root zone. Although cytokinin response markers were observed most frequently in the pericycle, they were also observed in the suberized endodermis (Fig. 2a and Extended Data Fig. 2b) but not in passage cells, which indicates an absent or attenuated cytokinin response in the latter cells (Fig. 2a). By observing the transcriptional expression patterns of most genes of the *Arabidopsis* response regulator (ARR) family, which contains negative (A-type) and positive (B-type) transcriptional regulators of cytokinin signalling<sup>12–14</sup>, we found that repressive A-type *ARR3* and *ARR6*, as well as the B-type *ARR14*, were expressed in passage cells; suberized endodermal cells, however, showed no expression of A-type ARRs (Extended Data Fig. 2c, d). This demonstrates that passage cells have a distinct set of cytokinin-response regulators and possibly explains their attenuated cytokinin response. Our inability to detect ARRs in suberized endodermis might be due to their low abundance in these cells or the fact that not all ARRs were represented in our marker set. Using the standard DR5 reporter, we detected auxin signalling only in vasculature and tissues surrounding lateral root primordia (Fig. 2b and Extended Data Fig. 2a). Using an improved version of the auxin reporter<sup>15</sup>, however, we observed additional signals that were restricted to xylem-pole endodermal cells but were not exclusive to passage cells (Fig. 2b). Passage cells are therefore associated with differential auxin and cytokinin responses within the circumference of the late endodermis.

Germinating seedlings on auxin increased the number of passage cells, but only at concentrations that also affected root growth (Fig. 2c and Extended Data Fig. 3). By contrast, cytokinin decreased passage-cell numbers even at concentrations that did not affect root growth (Fig. 2c and Extended Data Fig. 3). ABA strongly promotes endodermal suberization, and caused enhanced and precocious deposition of suberin<sup>2</sup>. As both ABA and cytokinin decreased the number of passage cells (Fig. 2c), we investigated how the two hormones might be connected. Seedling transfer to ABA-containing, but not to cytokinin-containing, plates for 24 h led to passage-cell closure (Fig. 2d), which was already observable after 9 h (Extended Data Fig. 4). This indicates that ABA can act during the late stages of endodermal

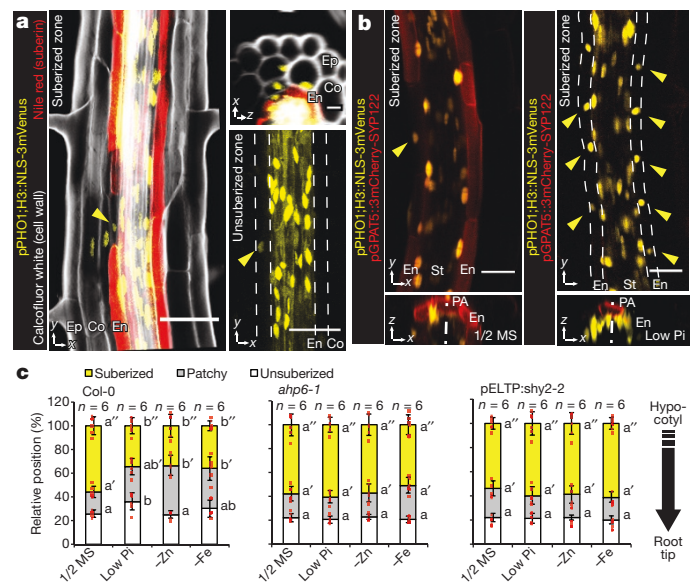


**Figure 4 | Passage cell-associated expression of *PHO1;H3*.** **a**, *PHO1;H3* reporter activity (NLS–3mVenus) in the suberized and unsuberized zones of differentiated endodermis. Cell walls (grey) visualized by calcofluor white and suberin (red) using Nile red. **b**, *PHO1;H3* expression in suberized zone of seedlings germinated on standard medium (1/2 Murashige and Skoog medium, 1/2 MS) or 10  $\mu$ M inorganic phosphate (low Pi). Suberized endodermis cells highlighted by *GPAT5* expression. Yellow arrowheads, passage-cell nuclei. **c**, Endodermal suberization in Col-0, *ahp6-1* and lines with repressed auxin signalling (through expression of *shy2-2*) in differentiated endodermis grown on standard medium, low Pi, or zinc (–Zn) or iron-deficient (–Fe) medium. Red dots, individual data points. For all stacked graphs, there are three measurements per root: unsuberized zone, white; patchy zone, grey; and suberized zone, yellow. PA, phloem axis. Bar graphs represent mean  $\pm$  s.d. Statistically significant differences between groups were tested using a post hoc Bonferroni-adjusted paired two-sided *t*-test. For more information regarding data plots, see Methods. In **a** and **b**, images are representative of 12 independent lines. *n*, independent biological samples. For individual *P* values, see Supplementary Table 2. Scale bars, 25  $\mu$ m.

development, whereas cytokinin affects meristematic patterning events. We observed that xylem-pole endodermal cell length is about half that of phloem-pole cells (Fig. 2e, f). Similar dimorphisms have previously been described for other species<sup>4</sup> and could arise from a cytokinin-dependent delay of exit from the division zone in xylem-pole-associated cells<sup>16,17</sup>.

Increasing concentrations of cytokinin increased the average length of xylem-pole-associated endodermal cells, which then approached the length of phloem-pole cells (Fig. 2f and Extended Data Fig. 5f). Consistent with its antagonistic action, auxin decreased the length of xylem-pole cells (Extended Data Fig. 5e); ABA did not affect endodermal cell length (Extended Data Fig. 5d). These data indicate that cytokinin causes a difference between xylem- and phloem-pole-associated endodermis in the transition zone; we use this difference as an early read-out of bisymmetric patterning within the endodermis (Extended Data Fig. 5g).

To test whether cytokinin and auxin act directly in the endodermis, we specifically overexpressed cytokinin- or auxin-signalling suppressors in all differentiating endodermal cells. Cytokinin inhibition caused an almost complete absence of suberization, as if all endodermal cells had acquired a passage-cell identity (Extended Data Fig. 5a–c and Extended Data Fig. 6a–d). This suppression of suberization could not be antagonized by ABA, supporting a model in which cytokinin signalling determines the responsiveness of endodermal cells to ABA (Extended Data Fig. 6e). Suberization persisted around lateral root emergence sites, which suggests that in these areas suberization is independent of cytokinin (Extended Data Fig. 5a). When inhibiting endodermal auxin signalling, we observed decreased passage-cell numbers (Extended Data Fig. 5b, c). We added a temporal control to these manipulations by using an oestradiol-inducible expression system<sup>18</sup>. A 29-h oestradiol induction



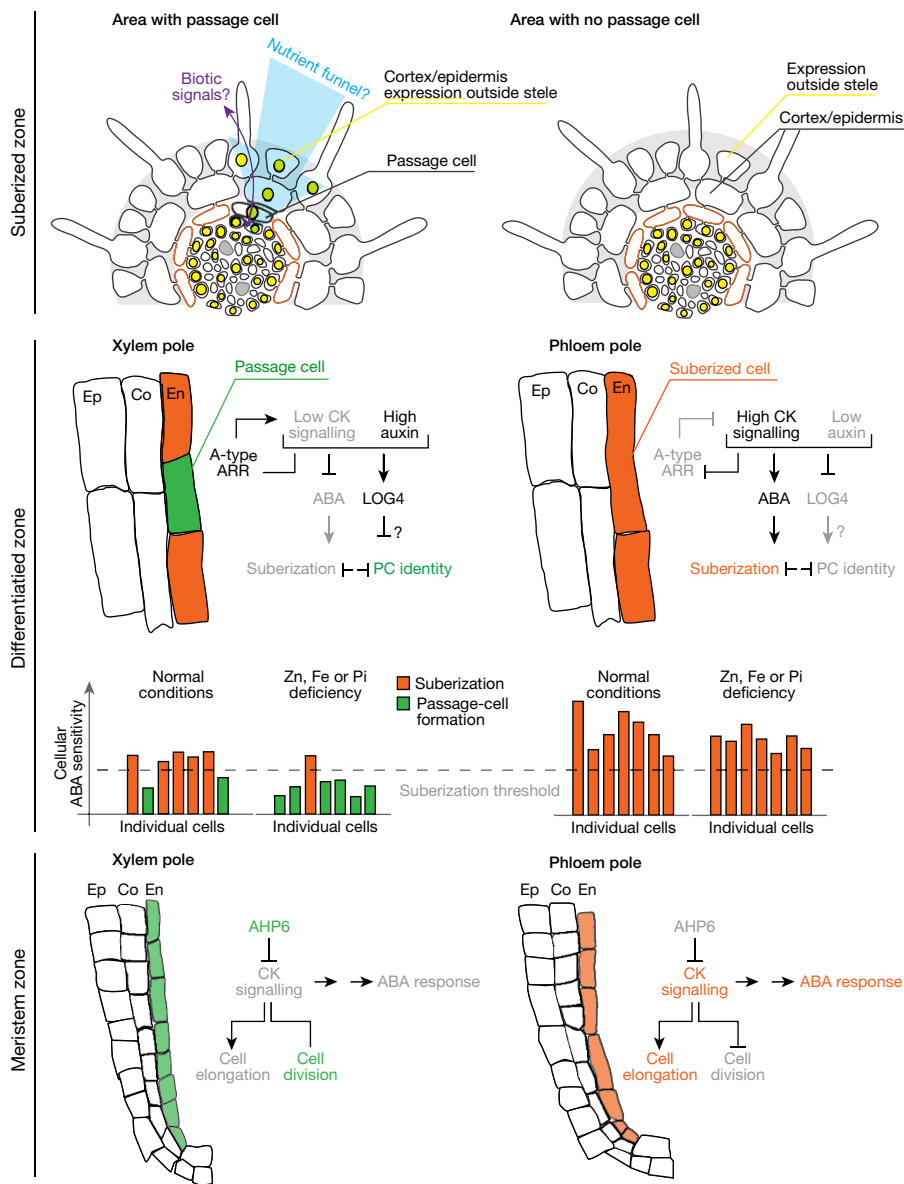


**Figure 5 | Overview of endodermis circumferential patterning and passage cell formation.** In the meristem zone, endodermal cells above the incipient xylem pole are exposed to AHP6 produced in the stele, which inhibits cytokinin signalling. This leads to prolonged division and thus shorter endodermal cells than in the phloem pole. Another output should be an overall lower response to ABA, through an as-yet unknown mechanism. In the differentiation zone, we hypothesize that the lower ABA response in xylem-pole endodermis stochastically causes some cells to be below the threshold for suberization. The unsuberized cells maintain low cytokinin signalling by expression of A-type ARR elements and also serve as—possibly auxin-dependent—cytokinin producers through the expression of LOG4. The status of ABA signalling is modulated by nutrient status, and thus passage cells can be closed given sufficiently high levels of ABA. In the fully suberized zone, the unsuberized xylem-pole-associated endodermal cells (passage cells) express specific genes with a domain that can spread to the cortex and/or epidermis, and serve to increase the area for uptake and/or to exchange signals with the environment (such as signals for biotic interactions). Nutrient stresses (zinc, iron or phosphate deficiencies) would increase the resistance of xylem-pole-associated endodermis cells towards ABA and lead to an increase in unsuberized cells, enabling increased transport-related gene expression. CK, cytokinin; PC, passage cell.

of AHP6–GFP did not affect suberization that was already established, or established passage cells, thereby confirming cytokinin application experiments (Extended Data Fig. 7). By contrast, auxin-repressor induction for 29 h reduced passage-cell numbers (Extended Data Fig. 7), which suggests that auxin signalling is also required to maintain passage-cell fate. Repressing ABA for 29 h led to an almost complete disappearance of suberin (Extended Data Fig. 7), which suggests that the strong suppression of ABA signalling interferes with maintenance of suberization, possibly by de-repressing ethylene signalling<sup>2</sup>. Having established the direct endodermal action of cytokinin, auxin and ABA in passage-cell formation, we sought to understand how spatial differences in cytokinin presence or perception might arise.

One regulator of cytokinin perception in the xylem pole is AHP6, the presence of which interferes with phospho-transfer reactions from receptors towards transcriptional regulators<sup>6</sup>. Although its transcription is confined to the stele, we found that a complementing AHP6–mVenus fusion diffuses into endodermal cells above the xylem pole (Fig. 3a and Extended Data Fig. 8a) where it may attenuate cytokinin signalling. To establish the relevance of this observation, we used a functional, non-mobile triple-mVenus AHP6 fusion<sup>19</sup>. Only the mobile single-mVenus fusion rescued passage-cell number and xylem-pole length of endodermal cells in *ahp6-1* mutants (Fig. 3c, d and Extended Data Fig. 8b). This was not due to the lower activity of the triple-m

Venus fusion, as the xylem patterning defects of *ahp6-1* were rescued to an even higher extent when a triple- rather than single-mVenus fusion was used (Fig. 3e). Thus, circumferential endodermal patterning and passage-cell differentiation relies on the movement of AHP6 from the stele into the endodermis.

In the stele, the cytokinin biosynthetic enzymes LOG3 and LOG4 turn xylem precursors into a source of cytokinin, which enhances signalling in neighbouring cells<sup>8</sup>. Interestingly, *log4*, but not *log3*, mutants showed lower passage-cell numbers (Fig. 3c and Extended Data Fig. 8g). *log4 ahp6-1* double mutants did not display a further reduction in passage cells (Extended Data Fig. 8g), which suggests that AHP6 and LOG4 act in a single pathway. The specificity of LOG4 can be explained by LOG3 transcription being restricted to the stele, whereas LOG4 is mainly expressed in xylem-pole-associated endodermal cells<sup>8</sup> (Fig. 3b). LOG4–GFP expression in differentiating, but not meristematic, endodermal cells rescued passage-cell numbers (Extended Data Fig. 8f), suggesting that LOG4 maintains passage-cell differentiation rather than being required for specification. Additionally, in *log4* mutants the length of xylem-pole endodermis is not affected (Extended Data Fig. 8b). Both AHP6 and LOG4 expression are reduced by cytokinin application<sup>6</sup> (Extended Data Fig. 8a, c) and this effect could explain the high sensitivity of passage-cell differentiation towards cytokinin. Combining *ahp6-1* with late endodermis-specific inhibition of auxin signalling further reduced



passage-cell differentiation (Extended Data Fig. 8e, h), which suggests that—in the absence of cytokinin repression—local auxin perception can partially maintain passage cells. None of the investigated mutants showed severe root developmental defects, although *ahp6-1* showed a slight reduction in lateral root emergence (Extended Data Fig. 3b).

The absence of suberization in passage cells could generate privileged sites for transport and communication. Despite the relatively small surfaces of passage cells, the uptake of some nutrients has previously been found to correlate with passage-cell numbers<sup>20–22</sup> and passage cells might include transporters that would be absent in suberized cells. Indeed, the phosphate efflux protein PHO1 was reported to be expressed in both stele and xylem-pole-associated endodermal cells<sup>22</sup>. To expand on this finding, we generated sensitive, triple-mVenus-based transcriptional reporter lines for the entire PHO1 family. Besides their expression in the stele, we found PHO1 and some homologues to be specifically expressed in passage cells (Fig. 4a and Extended Data Figs 9a–c). We additionally observed clusters of cortical and epidermal expression for many of these transport-mediating genes (Fig. 4a and Extended Data Fig. 9c). Counting cluster occurrence revealed their clear spatial association with passage-cell presence in the endodermis (Extended Data Fig. 9a). The association of cortical and/or epidermal expression of PHO1 family members with underlying passage cells could arise from stele-derived signals that exit through passage cells (Fig. 4a), and possibly funnel nutrients or biotic signals from epidermis towards xylem (Fig. 5). A similar role in communication has previously been proposed for hypodermal passage cells<sup>23</sup>.

Expression of PHO1 family members provides a positive definition of passage cells. PHO1;H3, the most easily visualized member of the family, shows expression in individual endodermal cells before the onset of suberization, which suggests that the specification of passage cells precedes suberization (Fig. 4a). We therefore used PHO1;H3 to assess whether the suppression of suberization by cytokinin correlates with expansion of the expression pattern of this gene. We found that endodermal cytokinin suppression leads to the general expression of PHO1;H3 in the endodermis, supporting the proposition that endodermal cells acquire passage-cell features on cytokinin repression (Extended Data Fig. 10b). Suppression of ABA signalling only expanded PHO1;H3 expression within xylem-pole endodermis, despite an equally strong suppression of suberization in all endodermal cells (Extended Data Figs 7, 10c), which again supports the notion that ABA acts at a later stage of endodermal development.

Finally, we investigated changes in PHO1;H3 expression under physiological stress conditions. Consistent with its putative role in phosphate transport, we found that phosphate deficiency suppressed suberization specifically in xylem-pole endodermis, and expanded PHO1;H3 expression into these cells (Fig. 4b). This response was abrogated in lines with enhanced cytokinin or suppressed auxin signalling (Fig. 4c). Expansion of PHO1;H3 expression in xylem-pole endodermis was similarly observed under conditions of zinc and iron deficiency, which have previously been shown to decrease suberization<sup>2</sup> and to enhance PHO1;H3 expression<sup>24</sup> (Fig. 4c and Extended Data Fig. 10d). This suggests that PHO1;H3 expansion is the result of an expansion of passage-cell occurrence, rather than a specific response to phosphate deficiency. qPCR analysis of PHO1;H3 expression corroborated our PHO1;H3 promoter fusion results (Extended Data Fig. 10e).

Our findings—that two endodermal cell types co-exist within roots, and possess distinct responsiveness to nutrients and hormones as well as different uptake and sensing potentials—have notable implications for current models of nutrient uptake in plants. Furthermore, the influence of isolated passage cells on neighbouring cells might explain how the small surfaces of these evolutionarily conserved cells could have important roles in nutrient transport or sensing (Fig. 5).

**Online Content** Methods, along with any additional Extended Data display items and Source Data, are available in the online version of the paper; references unique to these sections appear only in the online paper.

Received 1 August 2017; accepted 7 February 2018.

Published online 14 March 2018.

- Geldner, N. The endodermis. *Annu. Rev. Plant Biol.* **64**, 531–558 (2013).
- Barberon, M. *et al.* Adaptation of root function by nutrient-induced plasticity of endodermal differentiation. *Cell* **164**, 447–459 (2016).
- Peterson, C. A. & Enstone, D. E. Functions of passage cells in the endodermis and exodermis of roots. *Physiol. Plant.* **97**, 592–598 (1996).
- Kroemer, K. *Wurzelhaut, Hypodermis Und Endodermis Der Angiospermenwurzel* (*Bibl. Bot.* 59) (Erwin Nägele, 1903).
- Wu, H., Jaeger, M., Wang, M., Li, B. & Zhang, B. G. Three-dimensional distribution of vessels, passage cells and lateral roots along the root axis of winter wheat (*Triticum aestivum*). *Ann. Bot.* **107**, 843–853 (2011).
- Mähönen, A. P. *et al.* Cytokinin signaling and its inhibitor AHP6 regulate cell fate during vascular development. *Science* **311**, 94–98 (2006).
- Kurakawa, T. *et al.* Direct control of shoot meristem activity by a cytokinin-activating enzyme. *Nature* **445**, 652–655 (2007).
- De Rybel, B. *et al.* Integration of growth and patterning during vascular tissue formation in *Arabidopsis*. *Science* **345**, 1255215 (2014).
- De Rybel, B., Mähönen, A. P., Helariutta, Y. & Weijers, D. Plant vascular development: from early specification to differentiation. *Nat. Rev. Mol. Cell Biol.* **17**, 30–40 (2016).
- Bishopp, A. *et al.* A mutually inhibitory interaction between auxin and cytokinin specifies vascular pattern in roots. *Curr. Biol.* **21**, 917–926 (2011).
- Zürcher, E. *et al.* A robust and sensitive synthetic sensor to monitor the transcriptional output of the cytokinin signaling network in planta. *Plant Physiol.* **161**, 1066–1075 (2013).
- Hwang, I. & Sheen, J. Two-component circuitry in *Arabidopsis* cytokinin signal transduction. *Nature* **413**, 383–389 (2001).
- Sakai, H. *et al.* ARR1, a transcription factor for genes immediately responsive to cytokinins. *Science* **294**, 1519–1521 (2001).
- Mason, M. G. *et al.* Multiple type-B response regulators mediate cytokinin signal transduction in *Arabidopsis*. *Plant Cell* **17**, 3007–3018 (2005).
- Liao, C.-Y. *et al.* Reporters for sensitive and quantitative measurement of auxin response. *Nat. Methods* **12**, 207–210 (2015).
- Lavrekha, V. V., Pasternak, T., Ivanov, V. B., Palme, K. & Mironova, V. V. 3D analysis of mitosis distribution highlights the longitudinal zonation and diarch symmetry in proliferation activity of the *Arabidopsis thaliana* root meristem. *Plant J.* **92**, 834–845 (2017).
- Ioio, R. D. *et al.* A genetic framework for the control of cell division and differentiation in the root meristem. *Science* **322**, 1380–1384 (2008).
- Siligato, R. *et al.* Multisite gateway-compatible cell type-specific gene-inducible system for plants. *Plant Physiol.* **170**, 627–641 (2016).
- Besnard, F. *et al.* Cytokinin signalling inhibitory fields provide robustness to phyllotaxis. *Nature* **505**, 417–421 (2014).
- Harrison-Murray, R. S. & Clarkson, D. T. Relationships between structural development and the absorption of ions by the root system of *Cucurbita pepo*. *Planta* **114**, 1–16 (1973).
- Clarkson, D. T., Sanderson, J. & Russell, R. S. Ion uptake and root age. *Nature* **220**, 805–806 (1968).
- Hamburger, D., Rezzonico, E., MacDonald-Comber Petétot, J., Somerville, C. & Poirier, Y. Identification and characterization of the *Arabidopsis* PHO1 gene involved in phosphate loading to the xylem. *Plant Cell* **14**, 889–902 (2002).
- Sasse, J. *et al.* Asymmetric localizations of the ABC transporter PaPDR1 trace paths of directional strigolactone transport. *Curr. Biol.* **25**, 647–655 (2015).
- Khan, G. A. *et al.* Coordination between zinc and phosphate homeostasis involves the transcription factor PHR1, the phosphate exporter PHO1, and its homologue PHO1;H3 in *Arabidopsis*. *J. Exp. Bot.* **65**, 871–884 (2014).

**Supplementary Information** is available in the online version of the paper.

**Acknowledgements** This work was supported by funds to N.G. from an ERC Consolidator Grant (GA-N°: 616228 – ENDOFUN), an SNSF grant (31003A\_156261), an IEF Marie Curie fellowship (T.G.A.) and an EMBO Long-term postdoctoral fellowship (R.U.). B.D.R., W.S. and B.W. were funded by the Netherlands Organisation for Scientific Research (NWO; VIDI-864.13.001) and The Research Foundation - Flanders (FWO; Odysseus II GOD0515N). We thank A. Paradis and the Central Imaging Facility of the University of Lausanne for support; M. Yamazaki for providing constructs; B. Müller, D. Weijers and T. Vernoux for sharing material; A. Bishopp, A. P. Mähönen, D. Weijers, S. Sabatini, V. Grieneisen, Y. Helariutta and Y. Poirier for discussions; and A. Vjestica, C. Drapek, M. Marek and M. Barberon for input to the manuscript.

**Author Contributions** T.G.A. planned and conducted all experiments with input from N.G. and J.E.M.V. S.N. conducted initial experiments on PHO1 localization, R.U. created and tested inducible vectors, J.E.M.V. created and tested *shy2-2* lines, and B.D.R., W.S. and B.W. created and selected all ARR reporter lines. T.G.A. and N.G. wrote the manuscript. All authors commented on the manuscript.

**Author Information** Reprints and permissions information is available at [www.nature.com/reprints](http://www.nature.com/reprints). The authors declare no competing financial interests. Readers are welcome to comment on the online version of the paper. Publisher's note: Springer Nature remains neutral with regard to jurisdictional claims in published maps and institutional affiliations. Correspondence and requests for materials should be addressed to N.G. (niko.geldner@unil.ch) or T.G.A. (tonnigrube.andersen@unil.ch).

**Reviewer Information** Nature thanks H. Fukuda, Y. Helariutta and A. P. Mähönen for their contribution to the peer review of this work.

## METHODS

No statistical methods were used to predetermine sample size. The experiments were not randomized and investigators were not blinded to allocation during experiments and outcome assessment.

**Plant material and growth conditions.** For all experiments, seeds were surface-sterilized in 70% EtOH containing 0.05% Triton-X100, washed twice in 96% EtOH, plated on 1/2 MS (Murashige and Skoog medium) containing 0.8% agar (Duchefa) plates and vernalized at 4 °C for 2 days. Seedlings were grown vertically at 22 °C, under long-day conditions (18 h, 100  $\mu$ E). Unless stated otherwise, all microscopic analyses were performed on roots of 5-day-old seedlings. For hormone and oestradiol (Sigma) treatments, 4-day-old seedlings were transferred to 1/2 MS plates supplemented with hormones or DMSO (mock) for 1 day unless otherwise indicated. Zinc- and iron-deficiency studies were done as previously described<sup>2</sup>. For low phosphate studies, micro-agar containing 10  $\mu$ M phosphate (Duchefa Biochemie) and MS without phosphate (Caisson) was used. Plants were grown under 24 h light.

**Cloning.** The following published mutants and transgenic lines were used in this study: pCASP1::CDEF1<sup>25</sup>; *ahp6-1*<sup>6</sup>, pAHP6::AHP6-mVenus and pAHP6::AHP6-3mVenus<sup>19</sup>; *log3*, *log4* and *log34*, pLOG3::NLS3-GFP and pLOG4::NLS3-GFP<sup>8</sup>; pGPAT5::mCitrine-SYP122<sup>2</sup>; and pDonor221 containing ARR10<sub>EAR</sub><sup>26</sup>. Reporter constructs for ARR3–10, ARR14–17 and ARR21 were generated using LIC cloning<sup>27</sup>. pARR::NLS-2YFP plasmids were constructed for the other ARRs, using Gateway technology<sup>28</sup> (Life Sciences). The NLS-3mScarlet construct was obtained by DNA synthesis (Thermo Fisher Scientific) into a pDonor221 entry vector. To generate the oestradiol-inducible version of the ELTP promoter, we followed a previously published procedure based on a Gateway-compatible XVE system<sup>18</sup>. In brief, 464 bp of the 5'-UTR region of the ELTP (also known as EDA4) gene was cloned into XVE using a KpnI site using Infusion technology (Clontech). A list of primers and promoters can be found in Supplementary Table 1. Corresponding gene numbers listed in supplementary Table 1 or are as follows: *AB11*, At4g26080; *AHP6*, At1g80100; *CASP1*, At2g36100; *CDEF1*, At4g30140; *ELTP* (also known as *EDA4*), At2g48140; *GPAT5*, At3g11430; *LOG3*, At2g37210; *LOG4*, At3g53450; and *SYP122*, At3g52400.

**Imaging.** Confocal laser scanning microscopy experiments were performed on a Zeiss LSM 880 or a Leica SP8X microscope. All combinatorial fluorescence analyses were run as sequential scans. For fluorescence analysis of marker expression, a Clearsee-based<sup>29</sup> protocol was established. Cell walls were stained with calcofluor white (Polysciences) and suberin was stained with Nile red (Sigma). The following settings were used to obtain specific fluorescence signals: EGFP, excitation wavelength (ex): 470 nm, emission wavelength (em): 490–515 nm; mCitrine (with EGFP), ex: 525 nm, em: 530–550 nm; mCitrine (alone), YFP or mVenus, ex: 514 nm, em: 520–550 nm; dsTomato, ex: 561 nm, em: 565–595 nm; mCherry, ex: 594 nm, em: 600–650 nm; Nile red, ex: 561 nm, em: 600–650 nm; and calcofluor white, ex: 405 nm, em: 430–460 nm. fluorol yellow (Sigma) and xylem analysis was done on a Leica DM5000s fluorescence microscope using a GFP filter (ex: 470/40 nm dichroic 500 nm; em: BP 525/50 nm) for fluorol yellow, and a TX2 filter (ex: 560/40 nm dichroic 595 nm; em: 645/75 nm) in combination with differential interference contrast for xylem analysis.

**Transcriptional analysis.** Total RNA was extracted from 100 mg plant tissue using a Trizol-based PureLink RNA Mini Kit (Thermo Fisher Scientific), then DNase-treated and purified using RNeasy MinElute Cleanup Kit (Qiagen). Reverse transcription was done using a Superscript IV first strand synthesis system (Thermo Fisher Scientific). All steps were performed according to the manufacturers'

protocols. The PCR reaction was done on a Stratagene Mx3005P thermocycler using a MESA Blue Sybr Green kit. All transcripts are normalized to *UBQ10* expression (see Supplementary Table 1).

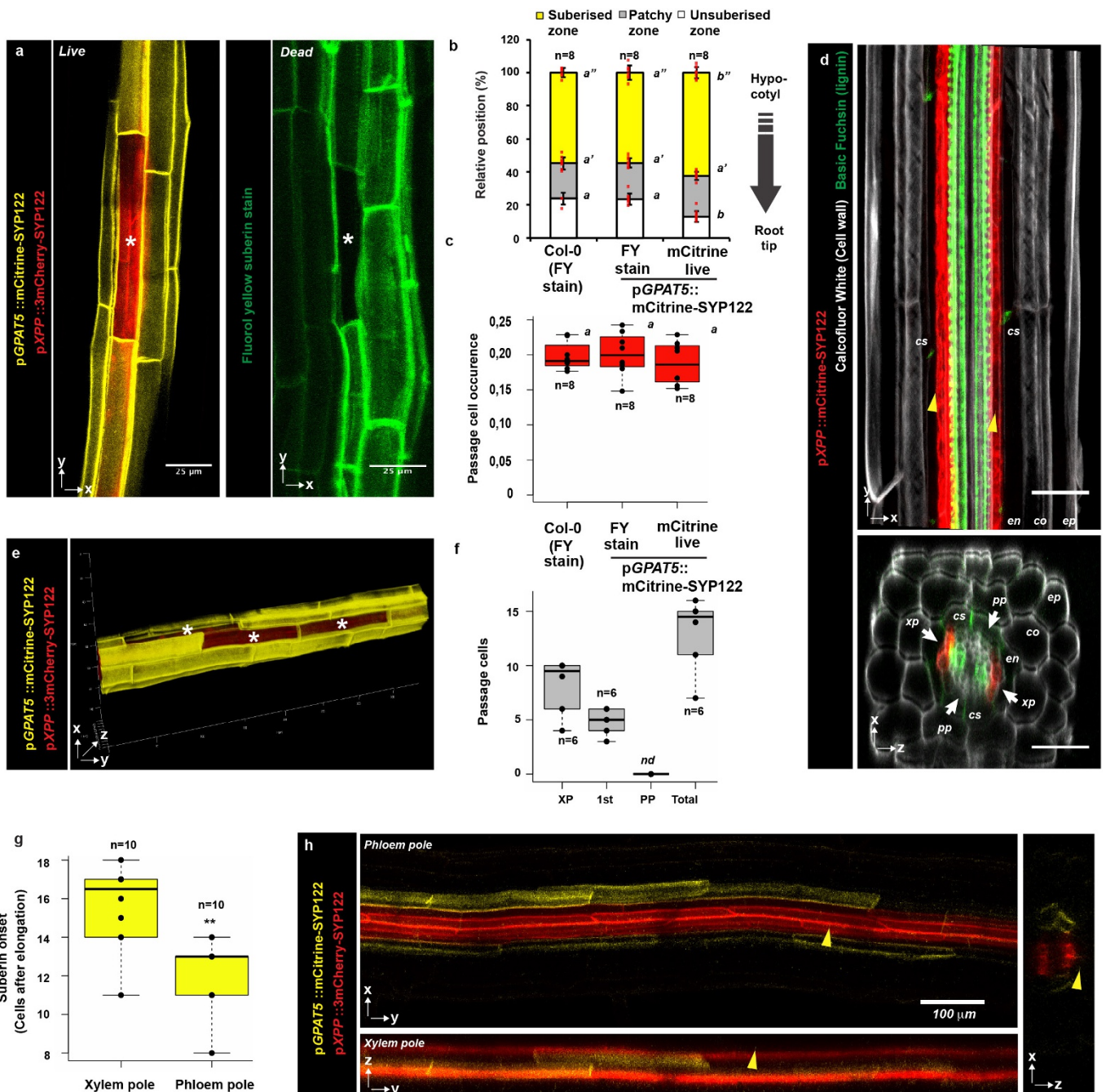
**Tissue staining and analysis.** Unless otherwise noted, suberin lamellae were observed after fluorol-yellow staining as previously described<sup>2,25,30,31</sup>. Suberin patterns were observed and counted from the hypocotyl junction to the onset of endodermal cell elongation. Three distinct patterns were considered: (1) continuous suberin lamellae; (2) patchy suberin lamellae (corresponding to the area in which individual cells are suberized); and (3) unsuberized cells (corresponding to the youngest part of the root). Passage cells were determined only in the zone containing continuous suberin lamellae. Passage-cell occurrence was obtained by counting the total number of passage cells in both xylem poles, divided by the length (in cells) of the zone. For quantifying the severity of *ahp6-1* xylem defects, the number of xylem-pole-associated endodermal cells above the defective xylem strand were counted, and related to total number of endodermal cells above each strand. Five-day-old roots were cleared using Clearsee<sup>29</sup> and stained with basic Fuchsin (Sigma) overnight, as previously reported<sup>32</sup>.

**Statistics and reproducibility.** All statistical analyses were done in the R environment<sup>33</sup>. For multiple comparisons between genotypes, a one-way ANOVA was performed with a Bonferroni-adjusted ad hoc pairwise two-sided *t*-test. Groups in which differences gave a *P* value lower than 0.05 were considered significantly different. Binary comparisons were performed using a two-tailed Student's *t*-test in Microsoft Excel; *P* values below 0.01 were considered significantly different. All bar graphs represent mean  $\pm$  s.d. For all boxplots, the centre depicts the median and the lower and upper box limits depict the 25th and 75th percentile, respectively. Whiskers represent minima and maxima. Closed dots depict individual samples. In cases in which *n* > 10, open dots depict outliers. In all cases, individual biological samples are stated as *n*. All experiments, as well as representative images, were repeated independently at least three times. Individual *P* values for all statistical analyses can be found in Supplementary Table 2.

**Data availability.** All lines and data generated in this study are available from the corresponding authors upon request.

- Naseer, S. *et al.* Casparian strip diffusion barrier in *Arabidopsis* is made of a lignin polymer without suberin. *Proc. Natl Acad. Sci. USA* **109**, 10101–10106 (2012).
- Müller, B. & Sheen, J. Cytokinin and auxin interplay in root stem-cell specification during early embryogenesis. *Nature* **453**, 1094–1097 (2008).
- Wendrich, J. R., Liao, C.-Y., van den Berg, W. A. M., De Rybel, B. & Weijers, D. Ligation-independent cloning for plant research. *Methods Mol. Biol.* **1284**, 421–431 (2015).
- Karimi, M., Bleys, A., Vanderhaeghen, R. & Hilson, P. Building blocks for plant gene assembly. *Plant Physiol.* **145**, 1183–1191 (2007).
- Kurihara, D., Mizuta, Y., Sato, Y. & Higashiyama, T. ClearSee: a rapid optical clearing reagent for whole-plant fluorescence imaging. *Development* **142**, 4168–4179 (2015).
- Pfister, A. *et al.* A receptor-like kinase mutant with absent endodermal diffusion barrier displays selective nutrient homeostasis defects. *eLife* **3**, e03115 (2014).
- Roppolo, D. *et al.* A novel protein family mediates Casparian strip formation in the endodermis. *Nature* **473**, 380–383 (2011).
- Ursache, R., Andersen, T. G., Marhavy, P. & Geldner, N. A protocol for combining fluorescent proteins with histological stains for diverse cell wall components. *Plant J.* **93**, 399–412 (2017).
- R Development Core Team. *R: A Language And Environment For Statistical Computing* (R Foundation for Statistical Computing, 2015)

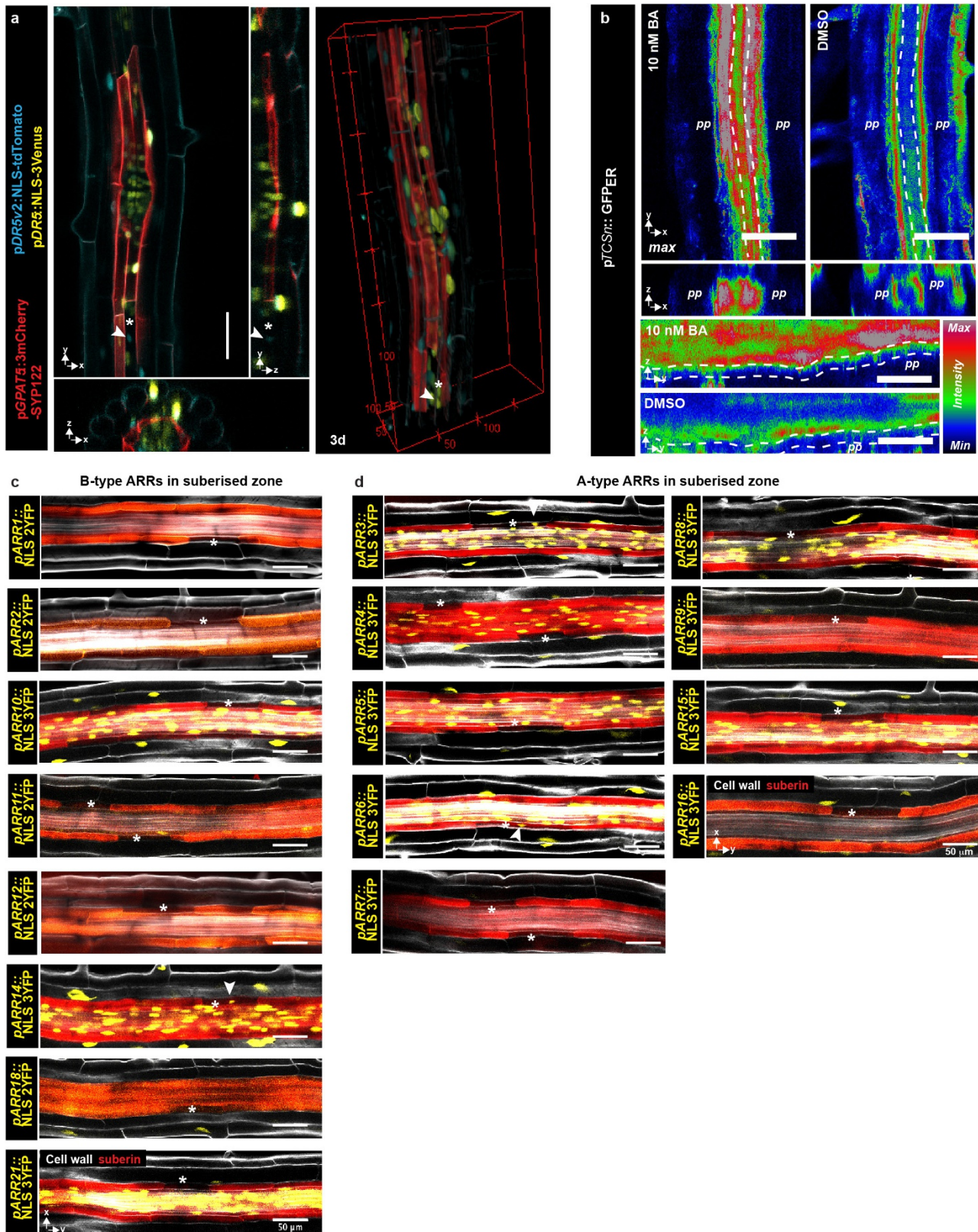




**Extended Data Figure 1 | Passage cells and suberization in *Arabidopsis*.**  
**a**, A single xylem-pole-associated passage cell surrounded by suberized cells; visualized in live imaging, by expression of the suberin biosynthetic gene *GPAT5* that drives expression of a plasma-membrane-localized mCitrine reporter (mCitrine-SYP122) (yellow, left) or by the suberin-specific dye fluorol yellow (green, right). In the left panel, the xylem-pole pericycle is highlighted using the promoter pXPP driving a 3mCherry reporter fused to the plasma-membrane-localized SYP122 (3mCherry-SYP122). Note that the fluorol-yellow protocol requires heating the sample to 70 °C, and is incompatible with fluorescent protein detection.  
**b**, Comparison of endodermal suberization in Col-0 and in plants expressing the *GPAT5*-based reporter, determined either by the suberin-specific dye fluorol yellow or live mCitrine expression, respectively. Red dots, individual data points.  
**c**, Comparison of passage-cell occurrence in Col-0 and in plants expressing the *GPAT5*-based reporter, determined either by the suberin-specific dye fluorol yellow or live mCitrine expression. Dots, individual data points.  
**d**, Expression of a plasma-membrane-localized mCitrine-SYP122 marker (red) driven by the xylem-pole-specific promoter pXPP, in the zone of protoxylem onset. Roots were cleared using ClearSee and stained with basic fuchsin (green) and

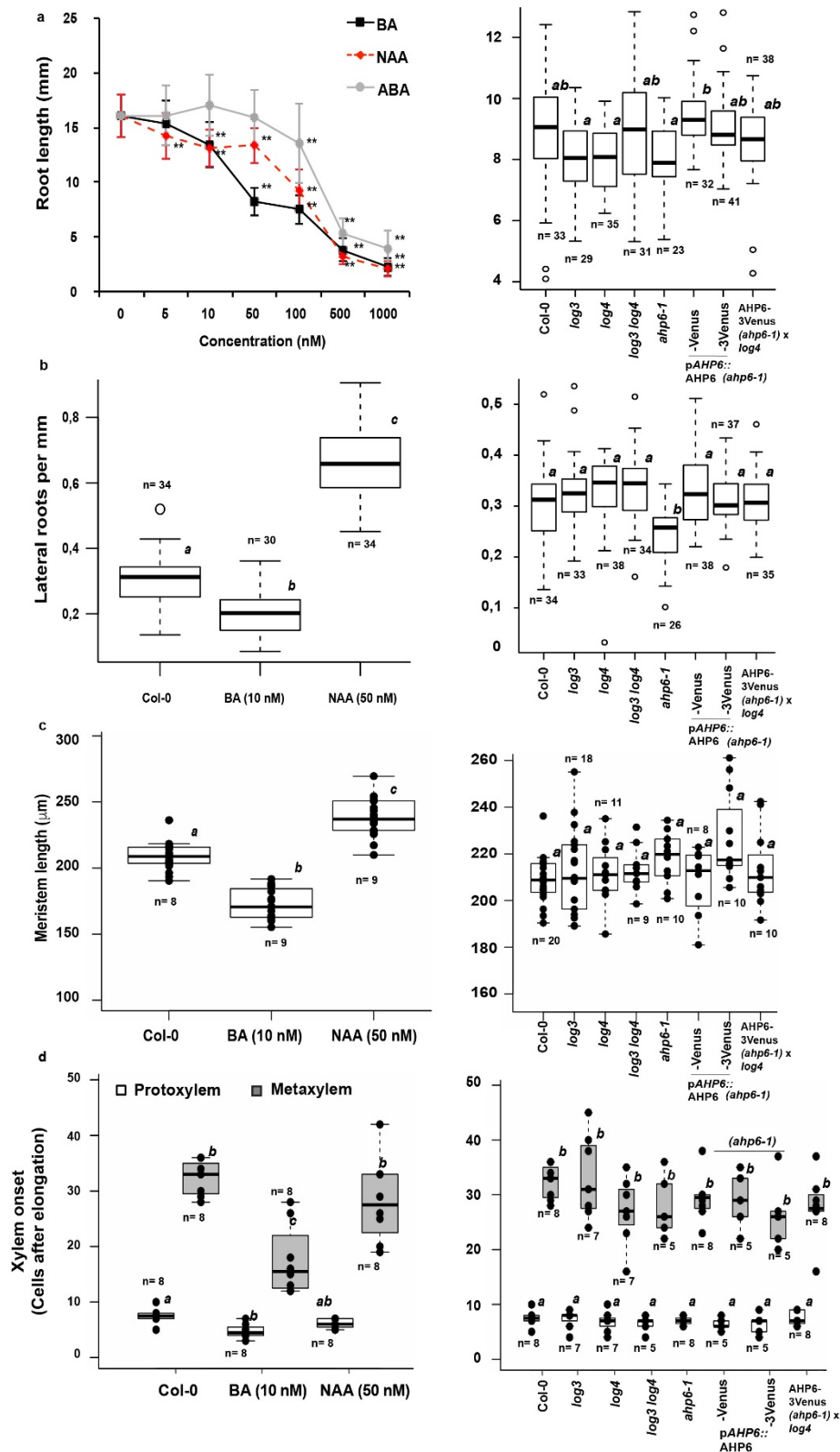
calcofluor white (grey)<sup>32</sup>. **e**, Radial- and longitudinally connected passage cells in the xylem pole of the suberized zone. **f**, Direct quantification of passage cells residing directly above xylem pole (XP), first side cell to the xylem pole (1st) or phloem pole (PP) in five-day-old Col-0 plants. Dots, individual data points. **g**, Quantification of the onset of endodermal suberization in the phloem and xylem poles of roots expressing markers as in **a**. Dots, individual data points. **h**, Representative images of the patchy zone of endodermal suberization in the phloem and xylem poles of roots used for quantification in **f**. Yellow arrowheads, xylem pole; asterisks, passage cells. cs; Casparian strip, FY; fluorol yellow. For all stacked graphs, there are three measurements per root: unsuberized zone, white; patchy zone, grey; and suberized zone, yellow. Bar graphs represent mean  $\pm$  s.d. and boxplots show median. Statistically significant differences between groups were tested using a post hoc Bonferroni-adjusted paired two-sided *t*-test. For more information on data plots, see Methods. **a** and **e** represent five independent lines; all stainings were repeated three times *n*, independent biological samples. \*\*\**P* < 0.01, two-tailed *t*-test. For individual *P* values, see Supplementary Table 2. Scale bars, 25  $\mu$ m, unless otherwise specified.





**Extended Data Figure 2 | Auxin and cytokinin signalling in the suberized root zone.** **a**, Activity of the auxin-signalling reporter DR5 (yellow) as well as the highly sensitive DR5v2 (blue) in an area of the suberized zone of a five-day-old root with an emerging lateral root. Suberized cells were visualized based on the suberin biosynthetic gene *GPAT5* driving expression of a plasma-membrane-localized 3mCherry-based reporter. **b**, Expression of endoplasmic-reticulum-localized GFP driven by the cytokinin signalling reporter *TCSn* in the phloem and xylem poles of 5-day-old roots in the suberized zone. Plants were either

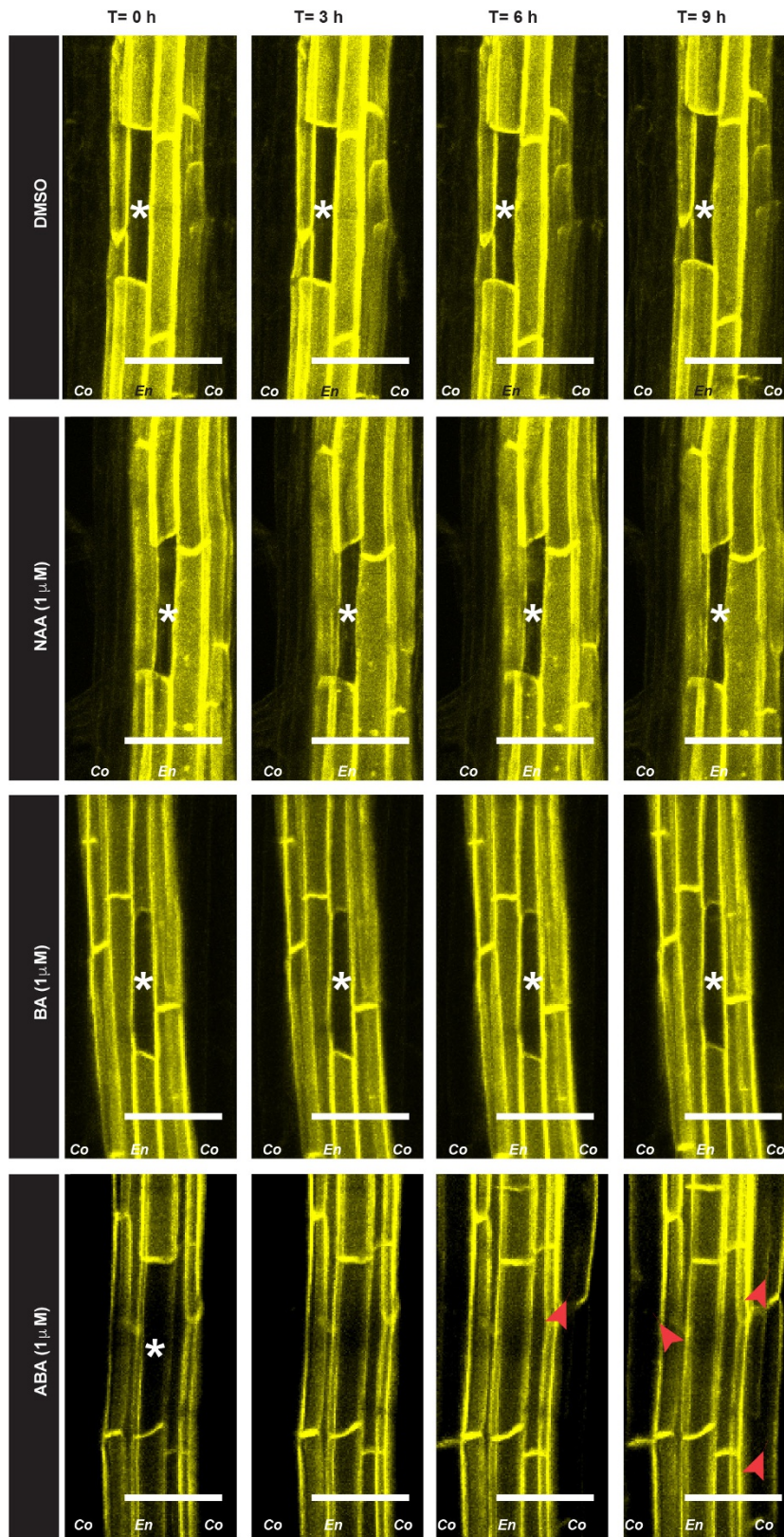
grown on plates containing 5 nM cytokinin (BA) or a mock treatment (DMSO). Punctured lines indicate the endodermis. **c**, Expression of B-type ARRs in the suberized endodermis of five-day-old roots, suberin and cellwalls are stained using a Clearsee protocol in combination with Nile red and calcofluor white, respectively<sup>32</sup>. **d**, Expression of A-type ARRs in the suberized endodermis of five-day-old roots, suberin and cell walls, as in **c**. All stainings were repeated three times. In **a** and **b**, images are representative of eight independent lines. White arrowheads, passage-cell nuclei. Asterisks, passage cells. Scale bars, 50  $\mu$ m.



**Extended Data Figure 3 | Phenotypic analysis of hormone-treated plants and mutants.** **a**, Root length of five-day-old plants either germinated on increasing concentration of cytokinin (BA), auxin (NAA) or abscisic acid (ABA) (left), or of the mutants used in this study (right). Open circles, outliers. **b**, Emerged lateral roots per mm of ten-day-old Col-0 roots germinated in presence of DMSO, 10 nM cytokinin (BA) or 50 nM auxin (NAA) (left), or of the mutants used in this study (right). Open circles, outliers. **c**, Length of the root apical meristem of five-day-old Col-0 plants germinated on either DMSO, 10 nM cytokinin (BA) or 50 nM auxin (NAA) (left), or of mutants used in this study (right). Dots,

individual data points. **d**, Onset of protoxylem and metaxylem after the elongation zone of five-day-old seedling germinated in presence of DMSO, 10 nM cytokinin (BA) or 50 nM auxin (NAA) (left), or of mutants used in this study (right). Dots, individual data points. Bar graphs represent mean  $\pm$  s.d. and boxplot centres show median. Statistically significant differences between groups were tested using a post hoc Bonferroni-adjusted paired two-sided *t*-test. For more information on data plots, see Methods. *n*, independent biological samples. In **a**,  $**P < 0.01$ , two-tailed *t*-test, *n* = 25 independent biological replicas for each treatment.

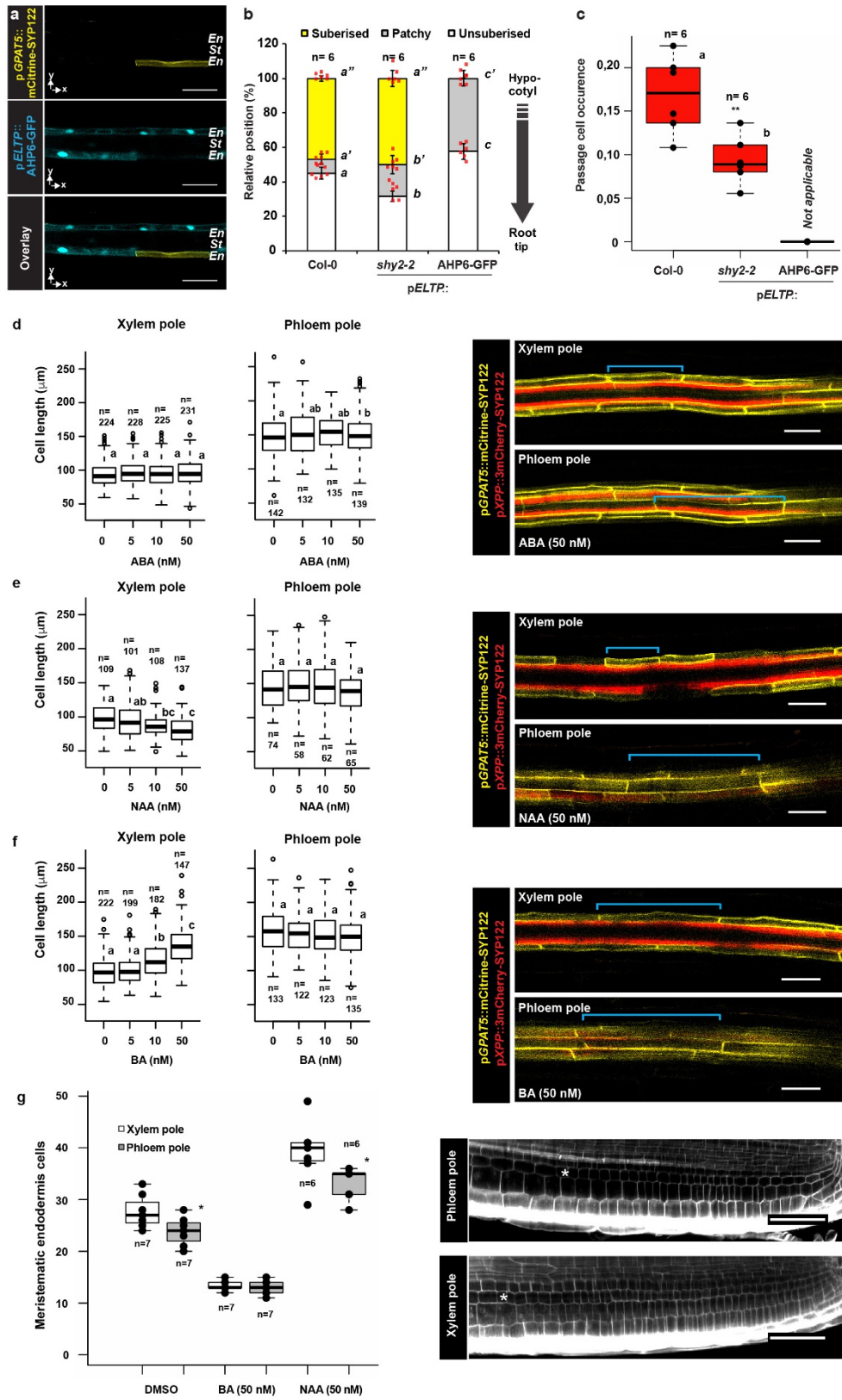




**Extended Data Figure 4 | Hormone-induced closure of passage cells.** Time-course analysis showing behaviour of passage cells, visualized by mCitrine-SYP122 driven by the promoter of the suberin synthesis marker gene *GPAT5* for 9 h on 1/2 MS medium containing DMSO, cytokinin (BA),

auxin (NAA) or abscisic acid (ABA). Red arrowheads point to ectopic suberization in the cortex on ABA treatment. Asterisks, passage cells. All time courses were repeated three times. Scale bars, 50 μm.

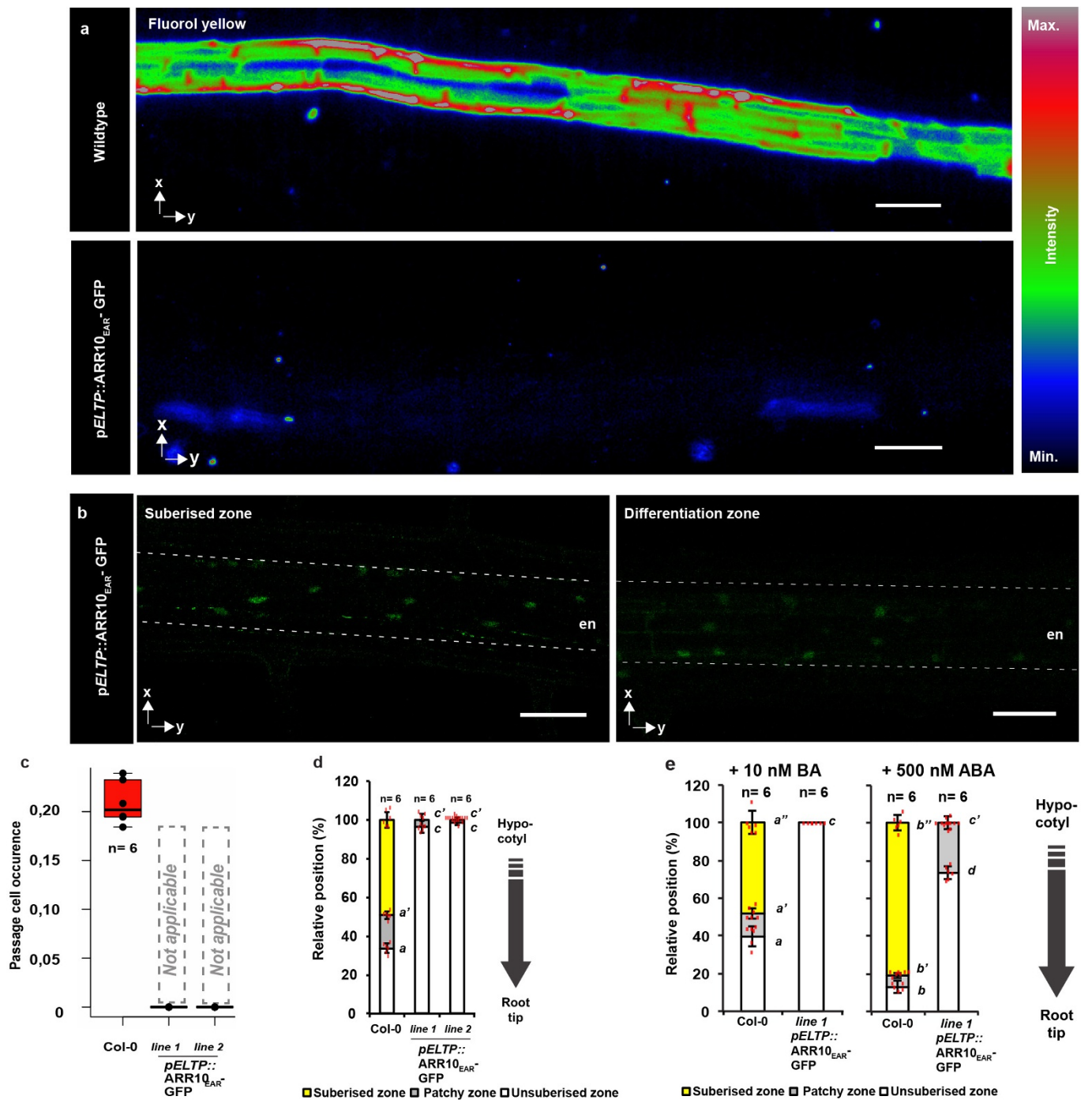




Extended Data Figure 5 | See next page for caption.

**Extended Data Figure 5 | Hormone-induced changes in endodermal cell lengths.** **a**, Expression of mCitrine-SYP122 driven by the *GPAT5* promoter (yellow), in the fully suberized zone in plants that express the dominant cytokinin-signalling inhibitor AHP6 fused to GFP in the differentiated endodermis using the *ELTP* promoter (blue). **b**, Endodermal suberization in five-day-old seedlings that express AHP6-GFP or the dominant auxin signalling repressor *shy2-2* in the differentiated endodermis. Red dots, individual data points. **c**, Occurrence of passage cells in five-day-old seedlings that express AHP6-GFP or the auxin signalling repressor *shy2-2* in the differentiated endodermis. Dots, individual data points. **d–f**, Length of suberized endodermal cells measured in the suberized zone of plants expressing pGPAT5::mCitrine-SYP122 and pXPP::3mCherry-SYP122 constructs. Open circles, outliers. Plants were grown for five days on 1/2 MS medium containing depicted concentrations of abscisic acid (**d**), auxin and naphthalene acetic acid (**e**), and cytokinin and benzyl adenine (**f**).

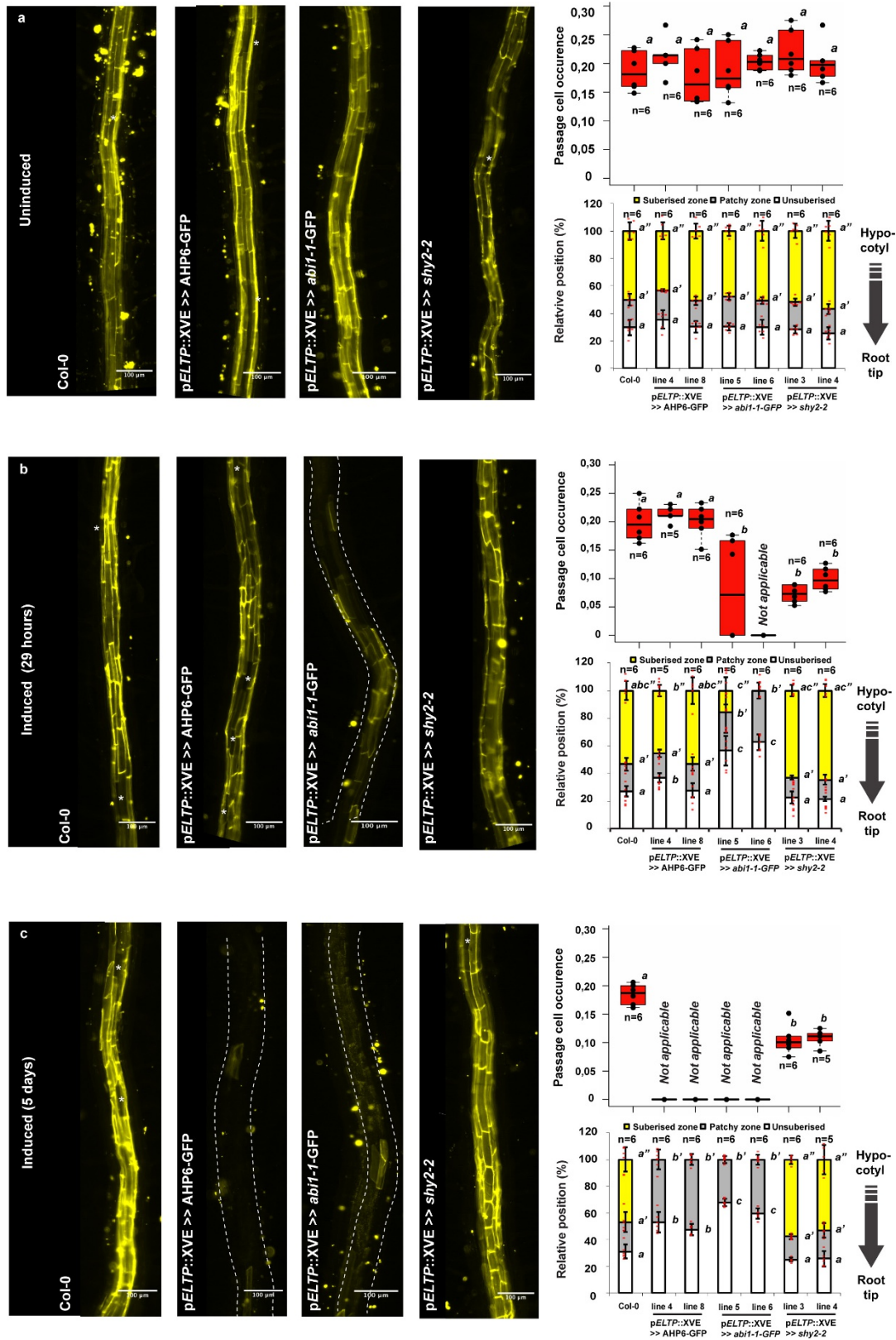
**g**, The number of meristematic cells in the phloem- and xylem-pole endodermis was counted in cleared roots stained with calcofluor white<sup>32</sup> to highlight cell walls. Dots, individual data points. For all stacked graphs, there are three measurements per root: unsuberized zone, white; patchy zone, grey; and suberized zone, yellow. Protoxylem or -phloem was used as a marker to identify the poles. Cells were counted from the quiescent centre to the onset of elongation. Asterisks, last cell of the division zone. Blue lines, lengths of individual cells. Bar graphs represent mean  $\pm$  s.d. and boxplot centres show median. Statistically significant differences between groups were tested using a post hoc Bonferroni-adjusted paired two-sided *t*-test. For more information on data plots, see Methods. In **a**, images are representative of 12 independent lines. In **g**, all stainings were repeated three times. *n*, number of measurements across 16 independent biological samples.  $^{***}P < 0.01$ , two-tailed *t*-test. Scale bars, 25  $\mu$ m.



**Extended Data Figure 6 | Manipulation of suberization through signalling repression.** **a**, Representative pictures of fluorol-yellow staining of suberin in lines expressing  $ARR10_{EAR}^{-}GFP$  in all differentiated endodermal cells, driven by the *ELTP* or *CASP1* promoters. **b**, Occurrence of passage cells in lines expressing  $ARR10_{EAR}^{-}GFP$  in all differentiated endodermal cells, using the *ELTP* and *CASP1* promoters. **c**, Behaviour of suberin in lines expressing  $ARR10_{EAR}^{-}GFP$  in all differentiated endodermal cells, using the *ELTP* and *CASP1* promoters. **d**, Behaviour of suberin in five-day-old plants expressing  $ARR10_{EAR}^{-}GFP$  in all differentiated endodermal cells, using the *ELTP* and *CASP1* promoters. Red dots, individual data points. **e**, Behaviour of suberin in five-day-old

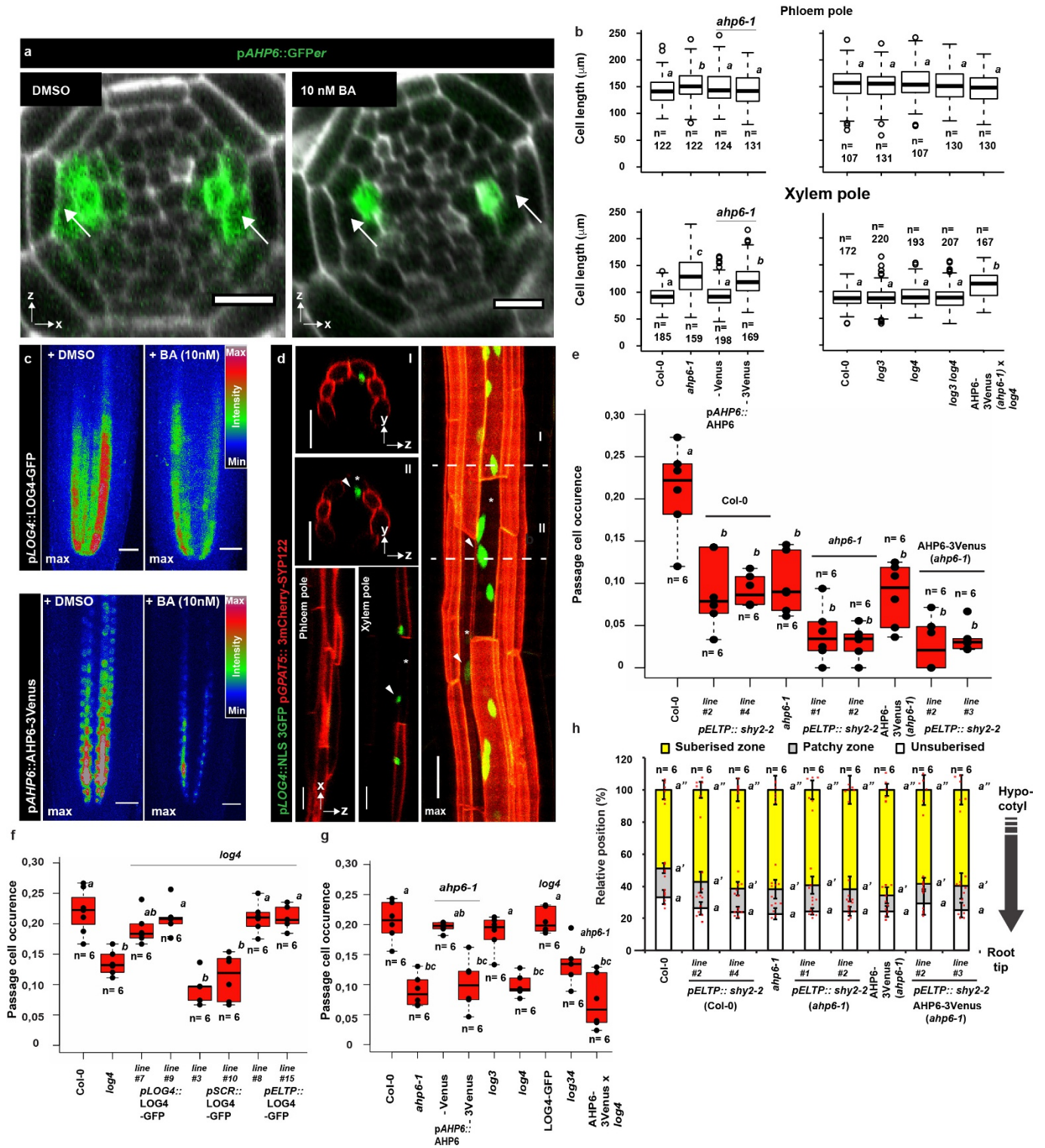
plants expressing  $ARR10_{EAR}^{-}GFP$  in all differentiated endodermal cells, using the *ELTP* and *CASP1* promoters, when plants were germinated on either cytokinin (BA) or abscisic acid (ABA). Red dots, individual data points. For all stacked graphs, there are three measurements per root: unsuberized zone, white; patchy zone, grey; and suberized zone, yellow. Bar graphs represent mean  $\pm$  s.d. and boxplots show median. Statistically significant differences between groups were tested using a post hoc Bonferroni-adjusted paired two-sided *t*-test. For more information on data plots, see Methods. In **b**, images are representative of nine independent lines. All stainings were repeated three times. *n*, independent biological samples. Scale bars, 50  $\mu$ m.





**Extended Data Figure 7 | Temporal control of suberin inhibition.** Expression of temporally controlled dominant inhibitors of cytokinin (AHP6-GFP), ABA (*abi1-1-GFP*) or auxin (*shy2-2*) signalling in the differentiated endodermis, using an oestradiol-inducible system (XVE)<sup>19</sup>. **a–c**, Fluorol-yellow staining (left) and quantification of passage cells (top right) and suberin (bottom right) in the late endodermis of plants grown on 1/2 MS medium containing DMSO for five days (a), plants grown for four days on 1/2 MS medium containing DMSO, then transferred to 5 μM oestradiol for 29 h (b) or germinated for five days on 1/2-MS-medium plates

containing 5 μM oestradiol (c). Asterisks, passage cells. All dots, individual data points. For all stacked graphs, there are three measurements per root: unsuberised zone, white; patchy zone, grey; and suberised zone, yellow. *n* represent biologically independent samples. Bar graphs represent mean ± s.d. and boxplot centres show median. Statistically significant differences between groups were tested using a post hoc Bonferroni-adjusted paired two-sided *t*-test. For more information on data plots, see Methods. In **a–c**, images are representative of nine independent lines. All stainings were repeated three times. *n*, independent biological samples. Scale bars, 100 μm.

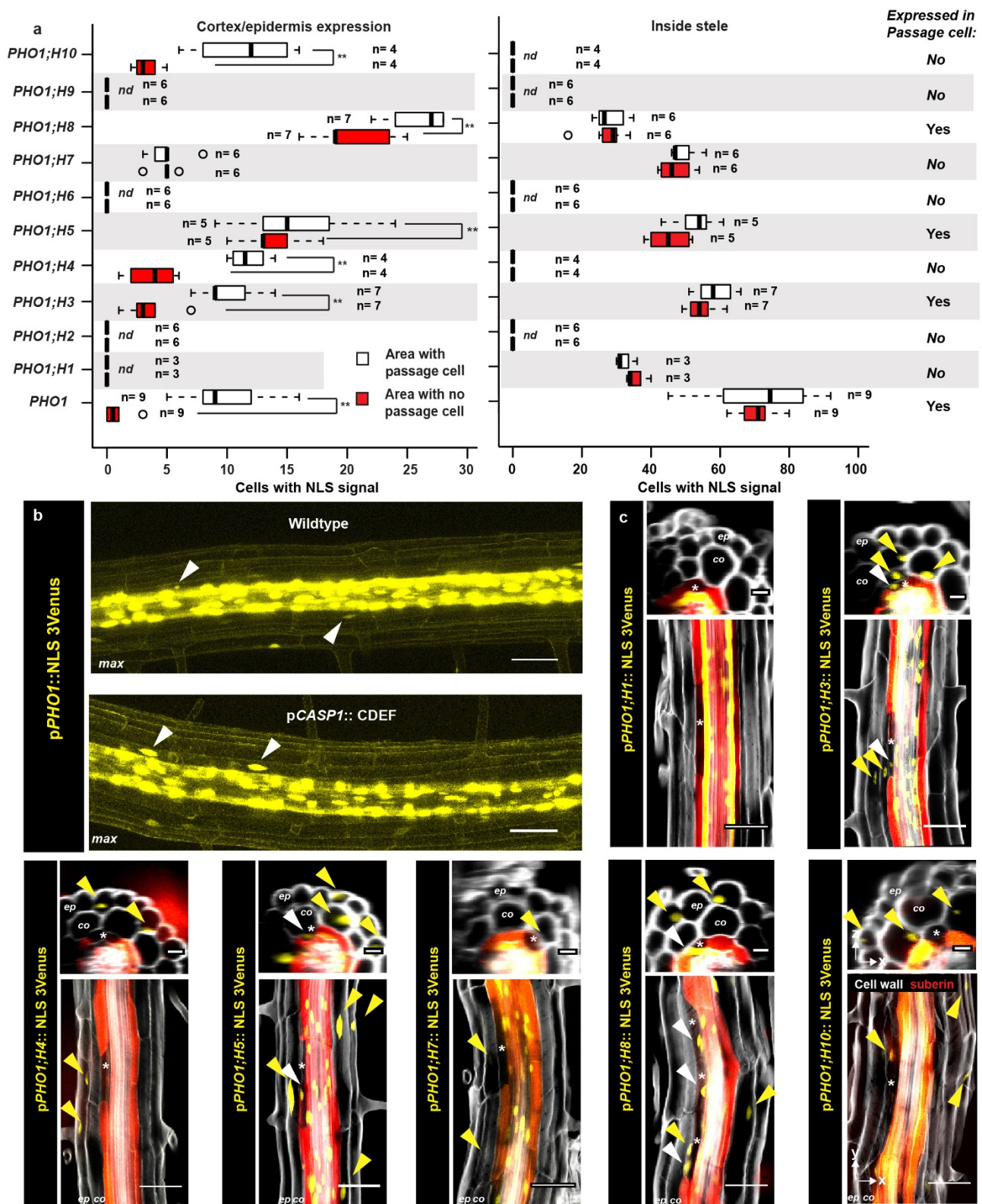


Extended Data Figure 8 | See next page for caption.

**Extended Data Figure 8 | Cytokinin-dependent formation of passage cells.** **a**, Expression of *AHP6* visualized by endoplasmic-reticulum-localized GFP (GFPer)<sup>19</sup>, in the root apical meristem of plants grown either in presence of a mock treatment (DMSO) or 10 nM cytokinin (BA). Arrows point to xylem-pole pericycle cells. **b**, Length of suberized endodermal cells in the phloem and xylem poles of five-day-old *ahp6-1* and *log* mutants, complementing lines and stacked mutants grown on 1/2-MS-medium plates. Data partly overlap with those in Fig. 3. Open circles, outliers. **c**, Expression of LOG4-GFP and AHP6-3mVenus driven by their native promoters, in the root apical meristem of plants grown either in presence of mock treatment (DMSO) or 10 nM cytokinin (BA). **d**, Expression of *LOG4* in the suberized zone of five-day-old seedlings visualized by the native *LOG4* promoter driving expression of an NLS-3GFP construct. Suberized endodermal cells were highlighted by expression of the suberin biosynthetic marker pGPAT5::3mCherry-SYP122. **e**, Occurrence of passage cells in lines with inhibited AHP6 diffusion in combination with repressed auxin signalling (through the expression of *shy2-2*) in the differentiated endodermis. Dots, individual data points. **f**, Passage-cell occurrence in the *log4* mutant complemented

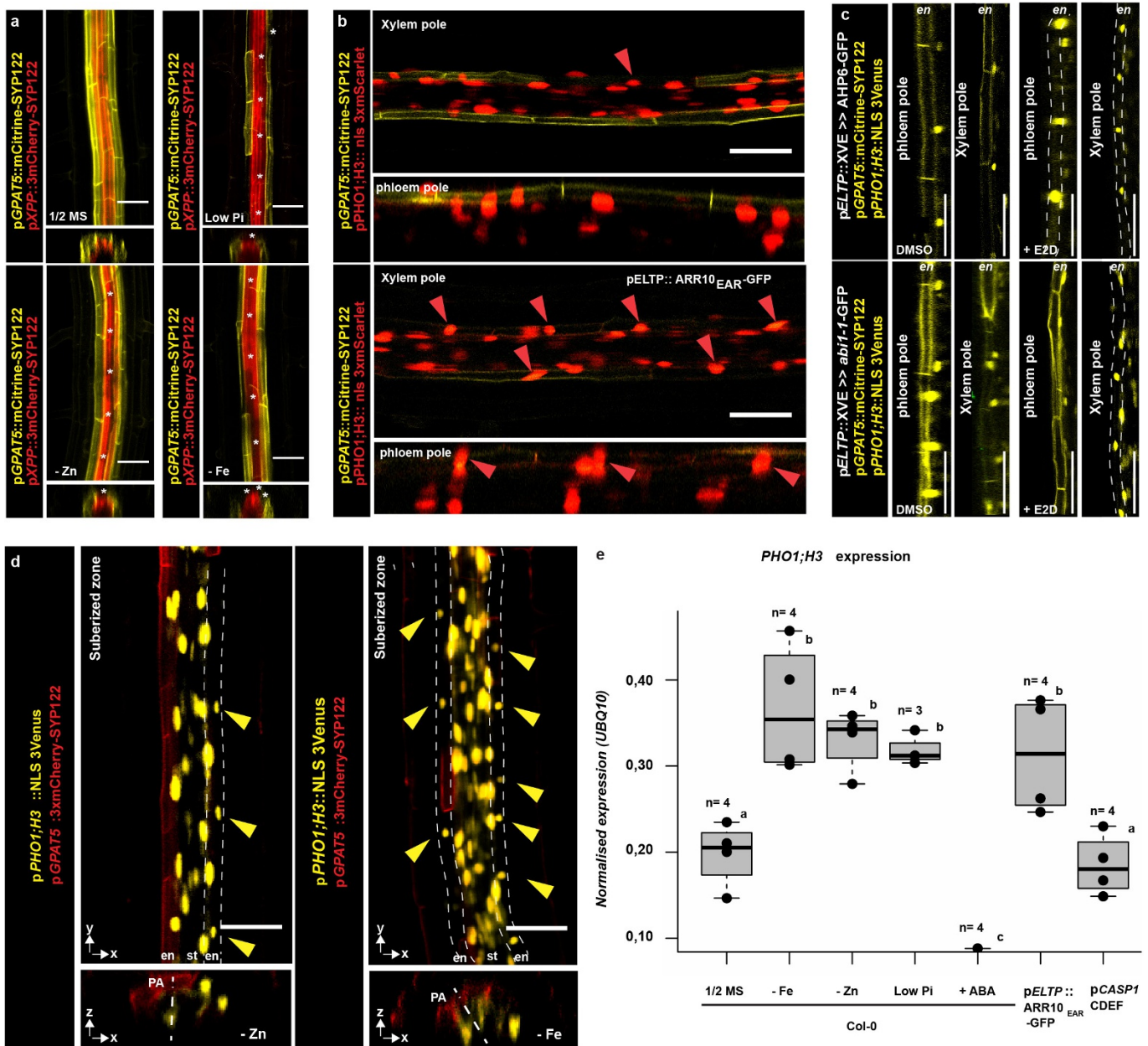
with a LOG4-GFP construct driven by either the native promoter (*pLOG4*), an early endodermis promoter (*pSCR*) or a differentiating endodermis promoter (*pELTP*). Dots, individual data points. **g**, Occurrence of passage cells in the suberized zone of five-day-old *ahp6-1*, *log* mutants and *ahp6 log* additionally complemented by non-mobile AHP6 to obtain endodermis-specific defects. Dots, individual data points. **h**, Behaviour of suberin in plants with or without inhibited auxin perception in the late endodermis grown on 1/2-MS-medium plates. Red dots, individual data points. For all stacked graphs, there are three measurements per root: unsuberized zone, white; patchy zone, grey; and suberized zone, yellow. Bar graphs represent mean  $\pm$  s.d. and boxplot centres show median. Individual letters show significantly different groups according to a post hoc Bonferroni-adjusted paired two-sided *t*-test. For more information on data plots, see Methods. In **c** and **d**, images represent eight independent lines. All stainings were repeated three times. *n*, independent biological samples. In **b**, *n* represents measurements across 16 biologically independent samples. Scale bars, 10  $\mu$ m (**a**) or 25  $\mu$ m (**c**, **d**).





**Extended Data Figure 9 | The PHO1 transporter gene family as marker for passage cells.** **a**, Expression of PHO1 family members in the cortex and/or epidermis (left) and inside the stele (right) within the suberized zone of five-day-old roots grown on 1/2 MS medium. Individual nuclei showing expression of the respective NLS reporter were counted in similar 3D stacks, taken either in a fully suberized area (red bars) or in an area containing one passage cell (white bars). Open circles, outliers. **b**, Expression of PHO1 in five-day-old seedlings in the late endodermis of wild type, or a suberin-degradation line with virtually absent suberin (pCASP1::CDEF1). **c**, Representative images of the expression of each member of the PHO1 family in roots of five-day-old seedlings,

highlighted by the NLS-3mVenus reporter. Seedlings were stained with Nile red for suberin and calcofluor white for cell walls. Scale bars in *x-z* projections represent 10  $\mu$ m. White arrowheads, passage-cell nuclei; yellow arrowheads point towards nuclei of cortex and/or epidermal cells. Asterisks, passage cells. n.d., not detected. Boxplot centres show median.  $**P < 0.01$ , two-sided *t*-test. For more information on data plots, see Methods. In **b** and **c**, images represent 15 and 11 independent lines, respectively. All stainings were repeated three times. *n*, independent biological samples. Unless otherwise stated, scale bars represent 25  $\mu$ m. For inserts, scale bars represent 10  $\mu$ m.



**Extended Data Figure 10 | Nutrient deficiency responses of suberization in the xylem pole.** **a**, Expression of the suberin marker *GPAT5* and the xylem-pole-pericycle marker *XPP* using a mCitrine-SYP122 or a 3mCherry-SYP122 plasma-membrane-anchored reporter, respectively. Plants were germinated for five days on 1/2 MS medium (1/2 MS), plates with low (10  $\mu$ M) inorganic phosphate (low Pi), no zinc (-Zn) or no iron (-Fe). Images representative of four independent lines. **b**, Expression of the suberin marker *GPAT5* and *PHO1;H3* using a mCitrine-SYP122 or a NLS-3mScarlet reporter, respectively, in the suberized zone of Col-0 plants or plants expressing the dominant cytokinin signalling repressor ARR10-GFP, in all differentiating endodermal cells. Each image is representative of eight independent lines. **c**, Expression of the suberin marker *GPAT5* and *PHO1;H3* using a mCitrine-SYP122 or a NLS-3mVenus reporter, respectively, in the suberized zone of plants expressing oestradiol-inducible (XVE) versions of the dominant cytokinin signalling repressor AHP6-GFP or the dominant ABA signalling repressor *abi1-1*, in all differentiated endodermal cells. Plants were grown for five days in presence of DMSO or 5  $\mu$ M oestradiol (+E2D), all treatments were repeated three times. Each image is

representative of five independent lines. **d**, Expression of *PHO1;H3* and the suberin marker *GPAT5* in roots of five-day-old Col-0 plants grown on 1/2 MS medium, plates containing no iron, no zinc or with low (10  $\mu$ M) inorganic phosphate. Each image is representative of nine independent lines. All treatments were repeated three times. **e**, Transcriptional analysis of *PHO1;H3* expression in roots of five-day-old Col-0 plants grown on 1/2 MS medium, plates containing no iron, no zinc or with low (10  $\mu$ M) inorganic phosphate, in plants expressing the dominant cytokinin signalling repressor ARR10-GFP in all differentiated endodermal cells, or in plants with strongly reduced suberin deposition by expression of a suberin-degrading enzyme (*pCASP1::CDEF*). Expression was normalized to that of *UBQ10*. Dots, individual data points. For all stacked graphs, there are three measurements per root: unsuberized zone, white; patchy zone, grey; and suberized zone, yellow. Asterisks highlight unsuberized xylem-pole endodermal cells. Boxplot centres show median. Statistically significant differences between groups were tested using a post hoc Bonferroni-adjusted paired two-sided *t*-test. For more information on data plots, see Methods. *n*, independent biological samples. Scale bars, 25  $\mu$ m.

## Life Sciences Reporting Summary

Nature Research wishes to improve the reproducibility of the work that we publish. This form is intended for publication with all accepted life science papers and provides structure for consistency and transparency in reporting. Every life science submission will use this form; some list items might not apply to an individual manuscript, but all fields must be completed for clarity.

For further information on the points included in this form, see [Reporting Life Sciences Research](#). For further information on Nature Research policies, including our [data availability policy](#), see [Authors & Referees](#) and the [Editorial Policy Checklist](#).

Please do not complete any field with "not applicable" or n/a. Refer to the help text for what text to use if an item is not relevant to your study. For final submission: please carefully check your responses for accuracy; you will not be able to make changes later.

### ▶ Experimental design

#### 1. Sample size

Describe how sample size was determined.

Generally sample size is chosen empirically, based on prior experience of how big a sample size must be to most probably obtain a reproducible, statistically significant result. Expected "size-of-effect" is taken into account.

#### 2. Data exclusions

Describe any data exclusions.

No data was excluded from this submission

#### 3. Replication

Describe the measures taken to verify the reproducibility of the experimental findings.

The data has been reliably reproduced

#### 4. Randomization

Describe how samples/organisms/participants were allocated into experimental groups.

No randomization was applied, but seedlings of different genotypes were grown together in same growth chambers and on the same plates.

#### 5. Blinding

Describe whether the investigators were blinded to group allocation during data collection and/or analysis.

blinding was not applied

Note: all in vivo studies must report how sample size was determined and whether blinding and randomization were used.

#### 6. Statistical parameters

For all figures and tables that use statistical methods, confirm that the following items are present in relevant figure legends (or in the Methods section if additional space is needed).

- | n/a                      | Confirmed   |
|--------------------------|---|
| <input type="checkbox"/> | <input checked="" type="checkbox"/> The <u>exact sample size</u> ( <i>n</i> ) for each experimental group/condition, given as a discrete number and unit of measurement (animals, litters, cultures, etc.)  |
| <input type="checkbox"/> | <input checked="" type="checkbox"/> A description of how samples were collected, noting whether measurements were taken from distinct samples or whether the same sample was measured repeatedly  |
| <input type="checkbox"/> | <input checked="" type="checkbox"/> A statement indicating how many times each experiment was replicated  |
| <input type="checkbox"/> | <input checked="" type="checkbox"/> The statistical test(s) used and whether they are one- or two-sided<br><i>Only common tests should be described solely by name; describe more complex techniques in the Methods section.</i>                              |
| <input type="checkbox"/> | <input checked="" type="checkbox"/> A description of any assumptions or corrections, such as an adjustment for multiple comparisons   |
| <input type="checkbox"/> | <input checked="" type="checkbox"/> Test values indicating whether an effect is present<br><i>Provide confidence intervals or give results of significance tests (e.g. <i>P</i> values) as exact values whenever appropriate and with effect sizes noted.</i> |
| <input type="checkbox"/> | <input checked="" type="checkbox"/> A clear description of statistics including <u>central tendency</u> (e.g. median, mean) and <u>variation</u> (e.g. standard deviation, interquartile range)   |
| <input type="checkbox"/> | <input checked="" type="checkbox"/> Clearly defined error bars in <u>all</u> relevant figure captions (with explicit mention of central tendency and variation)   |

See the web collection on [statistics for biologists](#) for further resources and guidance.



## ► Software

Policy information about [availability of computer code](#)

### 7. Software

Describe the software used to analyze the data in this study.

Image J  
Version 2.0.0-rc-64/1.51s  
Build e0512e3c19  
Microsoft Excel for mac 2011 Version 14.6.9 (160926)  
R  
Version 0.99.903

For manuscripts utilizing custom algorithms or software that are central to the paper but not yet described in the published literature, software must be made available to editors and reviewers upon request. We strongly encourage code deposition in a community repository (e.g. GitHub). *Nature Methods* [guidance for providing algorithms and software for publication](#) provides further information on this topic.

## ► Materials and reagents

Policy information about [availability of materials](#)

### 8. Materials availability

Indicate whether there are restrictions on availability of unique materials or if these materials are only available for distribution by a third party.

No restrictions

### 9. Antibodies

Describe the antibodies used and how they were validated for use in the system under study (i.e. assay and species).

No antibodies were used in this study

### 10. Eukaryotic cell lines

a. State the source of each eukaryotic cell line used.

No eukaryotic cell lines were used in this study

b. Describe the method of cell line authentication used.

*Describe the authentication procedures for each cell line used OR declare that none of the cell lines used have been authenticated OR state that no eukaryotic cell lines were used.*

c. Report whether the cell lines were tested for mycoplasma contamination.

*Confirm that all cell lines tested negative for mycoplasma contamination OR describe the results of the testing for mycoplasma contamination OR declare that the cell lines were not tested for mycoplasma contamination OR state that no eukaryotic cell lines were used.*

d. If any of the cell lines used are listed in the database of commonly misidentified cell lines maintained by [ICLAC](#), provide a scientific rationale for their use.

*Provide a rationale for the use of commonly misidentified cell lines OR state that no commonly misidentified cell lines were used.*

## ► Animals and human research participants

Policy information about [studies involving animals](#); when reporting animal research, follow the [ARRIVE guidelines](#)

### 11. Description of research animals

Provide all relevant details on animals and/or animal-derived materials used in the study.

No animals were used in this study

Policy information about [studies involving human research participants](#)

### 12. Description of human research participants

Describe the covariate-relevant population characteristics of the human research participants.

This study did not involve human research participants

# CORRECTIONS & AMENDMENTS

---

---

## CORRECTION

<https://doi.org/10.1038/s41586-018-0231-y>

## **Author Correction: Diffusible repression of cytokinin signalling produces endodermal symmetry and passage cells**

Tonni Grube Andersen, Sadaf Naseer, Robertas Ursache, Brecht Wybouw, Wouter Smet, Bert De Rybel, Joop E. M. Vermeer & Niko Geldner

Correction to: *Nature* <https://doi.org/10.1038/nature25976>, published online 14 March 2018.

In this Letter, owing to a copying error in Illustrator, the two centre panels in Extended Data Fig. 7a were identical. This error has been corrected online. The old, incorrect Extended Data Fig. 7 is shown in the Supplementary Information to this Amendment for transparency. Some typos ('occurence') in Figs. 1, 2 and 3 have also been corrected and the publication details for ref. 32 have been added.

**Supplementary Information** is available for this Amendment at <https://doi.org/10.1038/s41586-018-0231-y>.